POWER GAIN AND NOISE PERFORMANCE OF LINEAR ACTIVE TWO-PORT

By

Kotaro Hirano

January 1965

POWER GAIN AND NOISE PERFORMANCE OF LINEAR ACTIVE TWO-PORT

By

Kotaro Hirano

Degree: DOCTOR OF PHILOSOPHY

Major Subject: Electrical Communication Engineering

..... Chairman

ABSTRACT

This thesis, consisting of six chapters, investigates analitically and experimentally the power gain and the noise performance of linear active two-port, which is the key aspect of the design theory of amplifiers subject to the small signal,

Chapter I is the introduction to the field of linear active circuit theory in regard to this thesis, which includes the general introduction, the review of previous work and the presentation of the problem.

Chapter II deals with the unilateral gain of Mason which is an invariant of linear active two-port under the lossless transformation. In Section

2.2, the representations of unilateral gain in terms of Y, H, G, F and T parameters are shown. The unilateralized structure of two-port corresponds to the singular case of the characteristic gain matrix which is defined in Section 5.2. In Section 2.3, it is also shown by using the equivalent circuit that the unilateral gain of transistor is an invariant under the permutations of its grounding method. A kind of lossless transformation matrix for the permutation of the grounding method is given. The unilateral gain of the transistor calculated from the measured H parameters are shown on several operating conditions.

Chapter III presents the graphical design method of the high frequency transistor amplifiers by means of the Linvill chart and the power gain chart which is developed by the present author. In Section 3.2, the input and output immittance chart which can be used in finding out graphically the input (or output) immittance for the specified load (or source) immittance, and the load (or source) immittance for the specified input (or output) immittance. In Section 3.3, the Linvill chart is extended toward the region

of G_L Re $H_{22}<0$. In Section 3.4, the power gain chart which indicates the stable region of linear active two-port for the specified terminations and the power gain in this stable region, is developed. In Section 3.5, the graphical design method of high frequency transistor amplifiers is proposed by the use of the power gain chart and Linvill chart. In Section 3.6, the estimation of mismatching effect and the determination of bandwidth of the tuned amplifiers are considered on the families of circles for constant power transfer ratio. Finally, in Section 3.7, the verification of this design method is shown by the designing illustrations of high frequency transistor amplifiers.

Chapter IV is concerned with the measurement of the noisy components of the linear active two-port. In Section 4.2, the relations between several noisy components are formulated by means of the circuit parameters. In Section 4.3, the principle of measurement of the noisy components of the linear active two-port is presented. In Section 4.4, the measuring equipment for the noisy components of the linear active two-port which has been designed by the present author

is described. In Section 4.5, the measured results of the two-port noise of transistor is given.

Chapter V is the consideration on the exchangeable power gain and the exchangeable noise measure which have been defined by Haus and Adler as the criterion to estimate the gain and noise performance of the linear active two-port. In Section 5.2, the stationary values of the exchangeable power gain are obtained in terms of eigenvalues of the characteristic gain matrix which is defined in this thesis and the source impedances to realize the stationary gains are given by the ratios of the components of their eigenvectors. Then it is pointed out that those results have the formal similarity with the results for the exchangeable noise measure of Haus and Adler. In Section 5.3, the relation between the exchangeable power gain and noise measure is clarified on the source impedance plane. In Section 5.4, the physical meaning of the singular cases of the characteristic gain matrix and the characteristic noise matrix are considered; namely the former is singular for the unilateral two-port, and the later is singular for the two-port with one element and not restricted to

the negative resistance amplifiers reported by Penfield. In Section 5.5, it is proved that the eigenvalue of the characteristic gain matrix in Section 5.2 is the complex conjugate matched power gain at the input and output of the linear active two-port, and that the ratio of the components of its eigenvector is the source impedance to realize the matching power gain. In Section 5.6 through 5.9, by introducing the families of circles for constant exchangeable power gain and noise measure, the theory for the estimation of gain and noise performance in a general linear amplifier and for the designing its input circuit is developed from the view point of keeping the noise measure optimum. The exchangeable noise measure becomes the exchangeable excess noise figure for the linear amplifier with high gain. The approximation method of this case is presented in Section 5.10. Finally, in Section 5.11, the above mentioned theory is applied to the high frequency transistor amplifiers.

Chapter VI is the conclusion of this thesis.

ACKNOWLEDGMENT

The author has been indeed fortunate to conduct research under the guidance of his Research Advisers, Professor K. Aoyagi and Associate Professor T. Namekawa of Osaka University.

The author wishes to express his sincere acknowledgment to them for their patience, ever-stimulating guidances, discussions and encouragements.

The author thanks Professor S. Kumagai, Professor E. Sugata, Professor Y. Kasahara, Professor Z. Kitamura, Professor K. Itakura, Professor K. Miyawaki, Professor H. Ozaki and Associate Professor T. Fujisawa, all of Osaka University in his research field and served on the thesis committee, for their instructions on his doctoral research.

The author would like to take this opportunity to express his thanks to Professor J.G. Linvill of Stanford University, Professor H.A. Haus and Professor S.J. Mason of MIT, Professor H. Yanai of Tokyo University, Associate Professor K. Yanagisawa of Tokyo Institute of Technology and Dr. K. Kurokawa of

BTL for their informative discussions and encouragements and Dr. S. Kodama for his constructive suggestions in the preparation of this thesis.

Finally, the author thanks Mr. K. Okuno, Mr. M. Suyama, Mr. K. Kawamura, Mr. K. Kusunoki, Mr. K. Tanaka, Mr. Y. Konba and other members of Aoyagi laboratory for their helps in the series of experiments.

TABLE OF CONTENTS

CHAPTER I INTRODUCTION

1.1 General Introduction

The last few years have witnessed the remarkable progress of electrical engineering. At present there are many active devices available and still new devices are being developed; hence the establishment of general analysis of the linear active networks by means of circuit parameters is significant on two accounts. First, it provides a way for the unified treatment of the varied devices, and second it suggests a desired direction for the future development of such devices.

Though there are much work with regard to the passive circuit theory, we have still many problems in the field of active circuit theory which should be solved. The active two-port constructing an amplifier has been treated case by case; for instance, the transistor amplifiers have been designed by a cut-and-try method using the special equivalent circuit of the used transistor. This method is limited in application because it cannot be used for other devices.

On the other hand, the method of the circuit analysis for the linear active two-port, in which the circuit parameters are used, is often applied to the amplifiers. As the two-port, in this case, is characterized only by the terminal voltages and currents without the considerations of the inside structure of a two-port, the analized results remain valid independent of the kind of active device or utilized frequency. The analysis for imbeddings of load, source, feedback and so on needed for amplifiers can be carried out easily according to the known circuit theory. The circuit parameters of a two-port are represented in six forms, those are the Z, Y, H, G, F and T parameter representations, in which two values among the four values of input and output voltages and currents are selected as the independent variables. The used parameter in each analysis may be determined from the view point of the convenience of calculation, the easiness of measurement and the closeness to the physical meaning. In this thesis, the output current flow into the load immittance from the two-port is choosed as the positive direction in F and T parameter re-

presentations, and as the negative in other parameters. Each parameter in this thesis has a complex value.

From these viewpoints of present state, the general theory of linear active two-port by means of circuit parameters is investigated here, and the applications to transistor amplifiers are described in which the gain, noise, stability and bandwidth are taken into account. The unknown characters of the transfer power gain, the exchangeable power gain and the exchangeable noise measure are clarified and the basic design theory of amplifier is achieved.

1.2 Review of Previous Work

The brief review of the previous work on the power gain and noise performance of linear active two-port will be presented in this section.

There are many investigations concerning the power gain and stability of linear active two-port by Mason,[1]-[4] Pritchard,[5] Stern,[6] Bolinder,[7] Sharpe and Smith,[8] nd the quantities which characterize the performance of the two-port, such as, the invariant under the lossless transformation, the

maximum power gain, have been found.

The customary noise figure is not a good criterion to estimate amplifiers of low gain, because the noise figure can be lowered by the application of negative feedback but the noise performance of amplifier is not improved. Stimulated by the unilateral gain of Mason,[1],[2] Haus and Adler[9]-[14] found the invariant of linear noisy networks. The invariant is the optimum value of exchangeable noise measure which is suggested by them as a better characterization of amplifier noise performance. Penfield[15] found that the exchangeable noise measure of negative resistance amplifiers is independent of the practical lossless network used and must therefore always be equal to the optimum value. Kurokawa[16] proposed a different noise measure which includes the noise contribution from the load, and hence enabled us to compare the performance of two different amplifiers which are not necessarily optimized. Heffner[17] has given the fundamental noise limit of linear amplifiers by applying the uncertainty principle of quantum mechanics to the process of signal measurement.

Some efforts are performed by Linvill and

Schimpf[18]-[20] on the representations of the input and output power of an amplifier and the input and load immittance by means of the circle diagrams. The geometrical approach to the analysis of linear active two-port is significant on the designing an amplifier.[21] Gewertz[22] presented the geometric representation of the stability of reciprocal two-port, which is generalized to non-reciprocal two-port by Llewellyn.[23]

Van der Ziel[24]-[26] and Strutt[27] investigated the noise in transistor, but the method to measure the two-port noisy components of transistor has not been given.

1.3 Presentation of the Problem

This thesis investigates the power gain and the noise performance of linear active two-port by the use of circuit parameters. The main body of the thesis consists of two parts. In the first part, that is, Chapter II and III, the property of two-port is investigated in the absence of internal noise. The second part, that is, Chapter IV and V, is concerned with the property of two-port at the

presence of internal noise as in the preamplifier. The theory discussed in Chapter III and V is most significant in engineering, to which the unilateral gain and the measurement of noisy components of linear active two-port complement.

New results of the thesis may be summarized briefly as follows:

a) A kind of lossless transformation matrix for the permutation of connection is given. See Section 2.3.

b) The input and output immittance chart is obtained, which is used in finding the input (or output) immittance for a given load (or source) immittance. See Section 3.2.

c) The power gain chart which indicates the stable region of linear active two-port for the specified terminations and the power gain in this region, is presented. See Section 3.4.

d) A design method of high frequency transistor amplifiers is proposed by the use of the power gain chart. See Section 3.5.

e) The bandwidth of tuned transistor amplifiers is considered on the families of circles for constant

power transfer ratio. See Section 3.6.

f) The method to measure the noisy components of linear active two-port is found out. See Chapter IV.

g) The eigenvalues of the characteristic gain matrix and characteristic noise figure matrix which are defined in the thesis are the complex conjugate matching power gain and noise figure of linear active two-port and the source impedances to realize them are determined by the ratios of the components of their eigenvectors. See Section 5.2, 5.5 and 5.10.

h) The characteristic gain matrix of unilateral two-port is singular. The characteristic noise matrix is also singular for other two-port not restricted to the two-port with negative resistance which has been shown by Penfield. See Section 5.4.

i) The families of cirlces for constant exchangeable power gain, excess noise figure and noise measure are obtained on the complex source impedance plane. See Sections 5.7, 5.9 and 5.10.

CHAPTER II UNILATERAL GAIN

2.1. Preface

One of the desirable direction in active circuit theory is to find out the invariant under the lossless transformation which include the lossless feedback, the change of source impedance and the permutation of terminals. Mason has proved[1],[2] for linear active two-port that the unilateral gain

$$U = \frac{|Z_{12} - Z_{21}|^2}{4(\mathrm{Re}\,Z_{11}\,\mathrm{Re}\,Z_{22} - \mathrm{Re}\,Z_{12}\,\mathrm{Re}\,Z_{21})} \qquad (2.1)$$

of a two-port is an invariant for lossless reciprocal imbedding. In Eq. 2.1, Re is a real part. The unilateral gain, however, is unbound for lossy reciprocal imbedding if the two-port is active. The unilateral gain is further unbound for lossless nonreciprocal imbedding if the two-port is active. The proof of these two statements is given by Leine.[28]

The maximum power gain of unilateralized two-port by lossless imbedding or lossy reciprocal imbedding is expected in the quantity U calculated from the circuit parameters of the original two-port. For the unilateralized two-port, Z_{12}, Y_{12}, H_{12}, G_{12} and det

are reduced to zero. There are several papers on the subject of unilateralization[29]-[32] (including neutralization), and many possible neutralizing circuit has been presented.

In this chapter the unilateral gain is considered; namely other parameter representations of Mason's equation are given, and it is shown by the calculation using the equivalent circuit that the unilateral gain's of transistor under three grounding methods are equal each other. The permutation of grounding method is a kind of lossless imbedding. The lossless transformation matrix of grounding method is obtained for each permutation.

2.2 Unilateral Gain[33]

The complex conjugate matching power gain of the unilateral or the unilateralized two-port is represented in terms of each circuit parameter by

$$U = \frac{|Z_{21}|^2}{4 \operatorname{Re} Z_{11} \operatorname{Re} Z_{22}} \tag{2.2}$$

$$U = \frac{|Y_{21}|^2}{4 \operatorname{Re} Y_{11} \operatorname{Re} Y_{22}} \tag{2.3}$$

$$U = \frac{|H_{21}|^2}{4 \operatorname{Re} H_{11} \operatorname{Re} H_{22}} \tag{2.4}$$

$$U = \frac{G_{21}}{4 \mathrm{Re}\, G_{11}\, \mathrm{Re}\, G_{22}} \tag{2.5}$$

$$U = \frac{1}{2 \mathrm{Re}(F_{11} F_{22}^{*} + F_{12} F_{21}^{*})} \tag{2.6}$$

where * means the complex conjugate, which has the same form in Z, Y, H and G parameter representations. We have no its representation in T parameter. The source impedance to realize the complex conjugate matching power gain is given by Z_{11}^{*}, $1/Y_{11}^{*}$, H_{11}^{*}, $1/G_{11}^{*}$ and F_{11}^{*}/F_{21}^{*} $(= F_{12}^{*}/F_{22}^{*})$, and the corresponding load impedance is given by Z_{22}^{*}, $1/Y_{22}^{*}$, $1/H_{22}^{*}$, G_{22}^{*} and F_{22}^{*}/F_{21}^{*} $(= F_{12}^{*}/F_{11}^{*})$ respectively. The complex conjugate matching power gain is also obtained by the eigenvalue of the characteristic gain matrix defined in Section 5.2. The characteristic gain matrix is singular for the unilateral or the unilateralized two-port. These detail arguments are described in Chapter V.

As it is known that U of Eq. 2.1 is an invariant for lossless imbedding and is equal to the U of Eq. 2.2 using the new parameters of unilateralized two-port, U of Eq. 2.1 is the power gain matched at input

and output of the unilateralized two-port by lossless imbedding. The other parameter representations of Mason's unilateral gain are

$$U = \frac{|Y_{12} - Y_{21}|^2}{4(\mathrm{Re}\,Y_{11}\,\mathrm{Re}\,Y_{22} - \mathrm{Re}\,Y_{12}\,\mathrm{Re}\,Y_{21})} \tag{2.7}$$

$$U = \frac{|H_{12} + H_{21}|^2}{4(\mathrm{Re}\,H_{11}\,\mathrm{Re}\,H_{22} + \mathrm{Im}\,H_{12}\,\mathrm{Im}\,H_{21})} \tag{2.8}$$

$$U = \frac{|G_{12} + G_{21}|^2}{4(\mathrm{Re}\,G_{11}\,\mathrm{Re}\,G_{22} + \mathrm{Im}\,G_{12}\,\mathrm{Im}\,G_{21})} \tag{2.9}$$

$$U = \frac{|1 - \det F|^2}{2\,\mathrm{Re}(F_{11}F_{22}^* + F_{12}F_{21}^* - \det F)} \tag{2.10}$$

$$U = \frac{|1 - \det T|^2}{2\,\mathrm{Re}(T_{11}T_{22}^* + T_{12}T_{21}^* - \det T)} \tag{2.11}$$

where Im is a imaginary part, hence Z and Y, H and G, F and T parameter representations have similar forms respectively, that is, we have only three kinds of representations as the unilateral gain. In addition, if Y_{12}, H_{12}, G_{12} and det$\mathbf{S}$ are equal to zero, Eq. 2.7 through 2.10 are reduced to Eq. 2.3 through 2.6.

2.3 Unilateral Gain of Transistor

The unilateral gain of transistor for the grounded base configuration has been given by Mason.

The present author has calculated similary the unilateral gain of transistor for the grounded emitter and the grounded collector configurations using the equivalent circuit and has obtained the same results as for the grounded base configuration of Mason.

The lossless transformation matrix for the permutation of grounding methods which is represented in

$$Z' = n Z n_t \qquad t : \text{transposed} \qquad (2.12)$$

are given in Table 1,[34] where Z is the original impedance matrix, and Z' is the transformed impedance matrix. The transformation matrix between the grounded emitter and the grounded collector in Table 1 has been given by Mason and others have been obtained by the present author.

Table 1. Lossless transformation matrix for permutations of grounding methods.

	G.B.↔G.E.	G.E.↔G.C.	G.B.→G.C.	G.C.→G.B.
n	$\begin{pmatrix} -1 & 0 \\ -1 & 1 \end{pmatrix}$	$\begin{pmatrix} 1 & -1 \\ 0 & -1 \end{pmatrix}$	$\begin{pmatrix} 0 & -1 \\ 1 & -1 \end{pmatrix}$	$\begin{pmatrix} -1 & 1 \\ -1 & 0 \end{pmatrix}$

Finally, the curves of the unilateral gain of transistor calculated from the measured H parameters are shown in Figs. 2.1 and 2.2.

2.4 Summary of Chapter II

The complex conjugate matching power gain of unilateral two-port and the other parameter representations of Mason's unilateral gain are presented. It is shown by using the equivalent circuit that the unilateral gain of transistor for three grounding methods is the same value. The lossless transformation matrix with regard to the unilateral gain is given for each permutation of grounding method. Finally, the numerical values of unilateral gain for practical transistor are shown.

We do not know if the unilaterality is really necessary. We can design amplifiers that work well without being completely unilateral. Unilaterality is, however, desirable for the simplicity, both in theory and practice, and for the estimation of two-port characteristics.

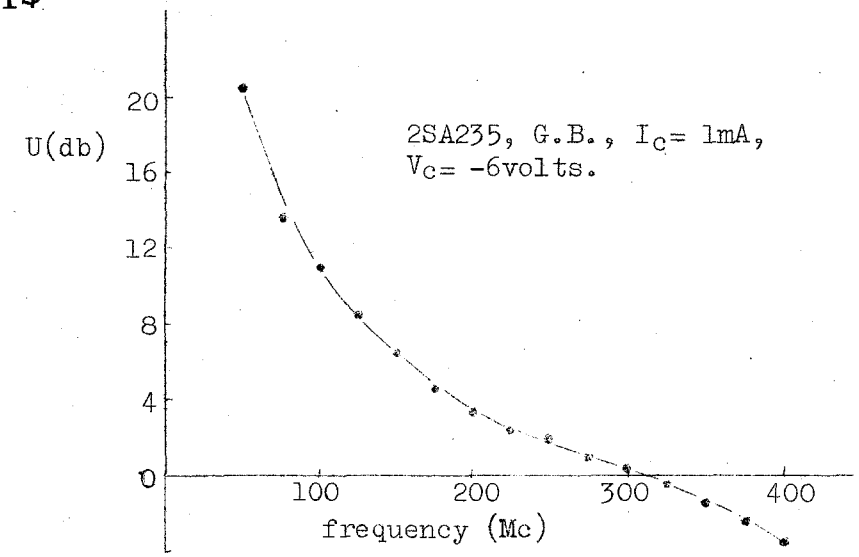

Fig. 2.1 Unilateral gain of transistor calculated from the H parameters, as dependent on frequency.

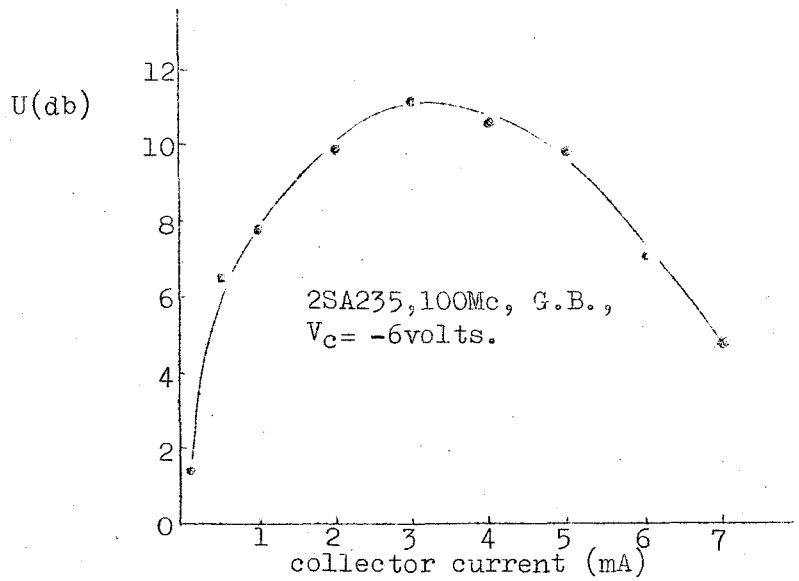

Fig. 2.2 Unilateral gain of transistor calculated from the H parameters, as dependent on collector current.

CHAPTER III POWER GAIN CHART AND ITS APPLICATION TO HIGH FREQUENCY TRANSISTOR AMPLIFIERS[35],[36]

3.1 Preface

The low frequency equivalent circuit of a transistor has been well established. We can, therefore, perform the general low frequency circuit analysis by the analogous conventional method used for vacuum tube amplifiers. The utilizable regions of transistor are still, expanding toward the VHF band and UHF band. Over the UHF band many kinds of equivalent circuits of transistor have been suggested. But there remain many problems: namely the complexity, the usable region and so on. The transistor amplifier in such high frequency bands is now designed by a cut-and-try method. Furthermore, many new semiconductor devices will be developed in the future and the circuit designers will make efforts to establish the equivalent circuits for these new devices. From these viewpoints, if the circuit designers persist in the design method of transistor amplifiers using an equivalent-circuit-approach, they will never be using an unified design method

because many more new devices are bound to be developed. The establishment of unified design method of the semiconductor amplifiers at high frequency by use of the circuit parameters is desirable for the prevention from disturbance in the design method of the new devices expected in future and for the unified interpretation of the semiconductor amplifiers.

Chapter III considers the transfer power gain and stability of a linear active two-port by the use of circuit parameters. The graphical method to find the input and output power, the input immittance and the terminated immittance of a given linear active two-port under the condition of the input matching has been developed by Linvill and Schimpf.[18)-(20)] However, a considerable amount of computations is still required to find the power gain and stable region, which are the most significant quantities for the circuit designers, and there is in need of simplification of the process. From the above viewpoints, this chapter points out the limit of the Linvill chart and an extended Linvill chart toward the region of $G_L Re H_{22} < 0$ is given. Then the power gain chart is described, by which the stability for specified

terminations (input matching), the transfer power gain inside of this stable region and the terminated immittance needed for specified power gain are obtained graphically by using it with the extended Linvill chart. In addition, a graphical design method of high frequency transistor amplifier is presented as one of the applications of this chart and the verification of this design method is confirmed by the experimental results. The ideas of the general input immittance chart and the families of circles for constant power transfer ratios are used complementally in the design of amplifiers.

3.2 Input and Output Immittance Chart of Linear Active Two-port[37]

The input immittance of a linear active two-port for specified load immittance can be obtained graphically by means of the Linvill chart and the input impedance overlay presented by Linvill. A different, yet simplified, graphical method of finding the input (or output) immittance of a linear active two-port for a given load (or source) immittance is described here in a more general way.

Figure 3.1 indicates a linear active two-port with the load immittance M_L and the source immittance M_S. The input immittance M_i and the output immittance M_o of linear active two-port are the functions of M_L and M_S as given by

$$M_i = M_{11} - \frac{M_{12} M_{21}}{M_{22} + M_L} \tag{3.1}$$

$$M_o = M_{22} - \frac{M_{12} M_{21}}{M_{11} + M_S} \tag{3.2}$$

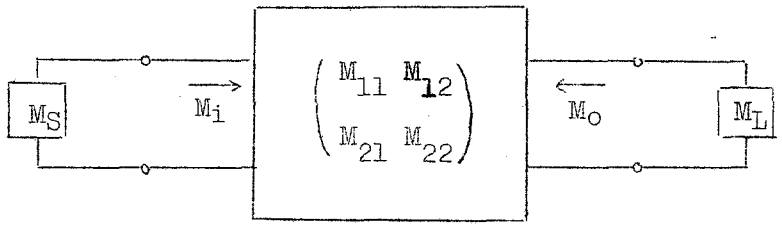

Fig. 3.1 An elementary system consisting of two-port, source and load.

First, the chart which indicates the input immittance for a given load immittance is considered. If we put

$$M_{11} - M_i = M_1 (= R_1 - jX_1) \tag{3.3}$$

$$M_{22} + M_L = M_2 (= R_2 + jX_2) \tag{3.4}$$

to Eqs. 3.1 and 3.2, it follows

$$R_1 = \frac{R_2 \, Re\, M_{12} M_{21} + X_2 \, Im\, M_{12} M_{21}}{R_2^2 + X_2^2} \tag{3.5}$$

$$X_1 = \frac{-R_2 \, \mathrm{Im}\, M_{12} M_{21} + X_2 \, \mathrm{Re}\, M_{12} M_{21}}{R_2^2 + X_2^2} \,. \tag{3.6}$$

From Eqs. 3.5 and 3.6 we have

$$\left(R_2 - \frac{\mathrm{Re}\, M_{12} M_{21}}{2R_1} \right)^2 + \left(X_2 - \frac{\mathrm{Im}\, M_{12} M_{21}}{2R_1} \right)^2 = \frac{|M_{12} M_{21}|^2}{4R_1^2} \tag{3.7}$$

$$\left(R_2 + \frac{\mathrm{Im}\, M_{12} M_{21}}{2X_1} \right)^2 + \left(X_2 - \frac{\mathrm{Re}\, M_{12} M_{21}}{2X_1} \right)^2 = \frac{|M_{12} M_{21}|^2}{4X_1^2} \tag{3.8}$$

making R_1 and X_1 be constant. The curves of Eqs.3.7 and 3.8 are families of circles with constant M_1 on the complex M_2 plane, and their loci of centers as M_1 varies are given by

$$X_2 = \frac{\mathrm{Im}\, M_{12} M_{21}}{\mathrm{Re}\, M_{12} M_{21}} R_2 \tag{3.9}$$

$$X_2 = -\frac{\mathrm{Re}\, M_{12} M_{21}}{\mathrm{Im}\, M_{12} M_{21}} R_2 \,. \tag{3.10}$$

The straight lines given by Eqs. 3.9 and 3.10 are orthogonal each other. The circles expressed by Eqs. 3.7 and 3.8 are obtained by rotating the chart of Fig. 3.2 by θ, where θ is specified by

$$\theta = \arg (M_{12} \cdot M_{21}) \,. \tag{3.11}$$

We can find M_i (or M_L) for the specified M_L (or M_i) by using Fig. 3.2.

The output (source) immittance of linear active two-port for a given source (output) immittance can be found similarly from this chart by putting

$$M_{11} + M_S = M_2 \qquad (3.12)$$

$$M_{22} - M_O = M_1 \qquad (3.13)$$

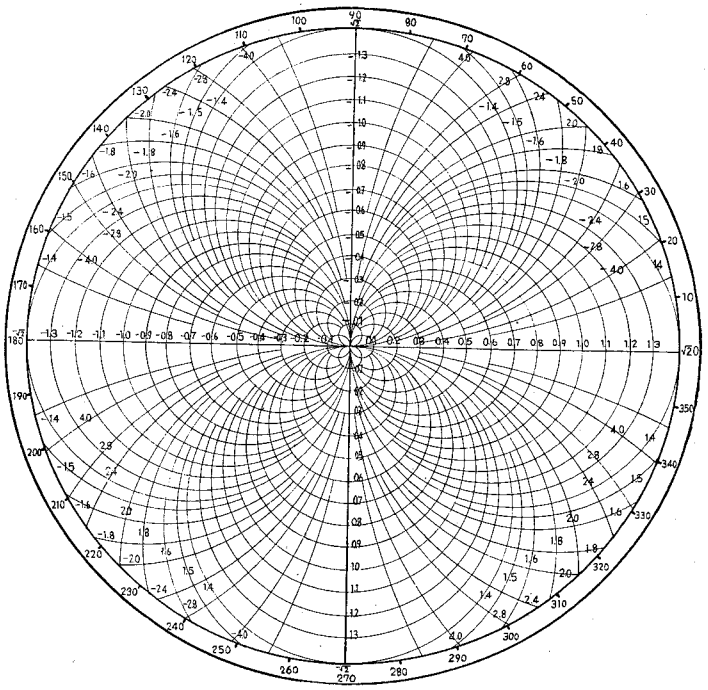

Fig. 3.2 Input and output immittance chart of linear active two-port.

The numerical example of finding the output impedance for the source impedance $Z_S = 46+22j(\Omega)$ by means of this chart is shown in the following. Z parameters of the used transistor (2SA235) at 100Mc of G.E., V_C=-12V, I_C=1mA are

$$\begin{pmatrix} Z_{11} & Z_{12} \\ Z_{21} & Z_{22} \end{pmatrix} = \begin{pmatrix} 58.2-4.25j & 25+j12.5 \\ 675+j550 & 525-525j \end{pmatrix} \Omega .$$

We have

$$Z_{12}Z_{21} = (1+2.22j) \times 10^4$$

$$|Z_{12}Z_{21}| = 2.44 \times 10^4$$

$$\theta = \arg (Z_{12} Z_{21}) = 66$$

$$Z_{11}+Z_S = 105 + j17.8.$$

If we choose R_2', X_2' in the range of

$$0 < R_2', \quad X_2' < \sqrt{2} ,$$

we have

$$R_2' = \frac{R_2}{100} = 1.05 \qquad X_2' = \frac{X_2}{100} = 0.178.$$

The readings on the input and output immittance chart are obtained from the point corresponding to (R_2', X_2') in the rectangular grid. Therefore

$$\frac{|Z_{12}Z_{21}|}{100R_1} = 1.9 \qquad \frac{|Z_{12}Z_{21}|}{100X_1} = -1.28$$

$$R_1 = 128, \qquad X_1 = -191$$

$$Z_o = Z_{22} - Z_1 = 497 - 815j \ (\Omega).$$

This is the output impedance of the transistor when the source impedance is $46+22j$ (Ω).

3.3 Input and Output Power, and Termination Immittances

The Linvill chart representing the terminations of linear active two-port and the charts indicating the input and output power for a given terminations

were first proposed by Linvill. In this section, the representations of the input and output power and the Linvill chart are described first using the notations of Linvill[18]-[20] as much as possible, in order to clarify the relation between them and the power gain chart which is developed in Section 3.4. Then the extended Linvill chart toward the region of $G_L \mathrm{Re}H_{22} < 0$ is given.

A linear active two-port with the source impedance $Z_S (=R_S+jX_S)$ and the load admittance $Y_L (=G_L + jB_L)$, has the specified input current and output voltage. As is shown in Fig. 3.3, the terminations of an active two-port are represented in the current and voltage sources specified by L and M.

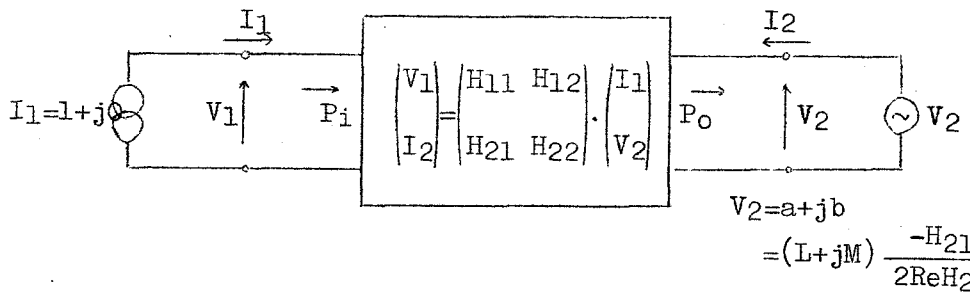

Fig. 3.3 Linear active two-port and terminating sources represented in L and M.

The representations of the input power P_i from the source to the two-port and that of the output power P_o from the two-port to the load have been given in terms of L and M. For unilateral two-port, $P_i = Re H_{11}$. The surface of P_i in the (L,M,P_i) space is a plane and the locus of P_i on the LM plane is given by

$$M = \frac{Re\, H_{12} H_{21}}{Im\, H_{12} H_{21}} L - \frac{2 Re\, H_{11} Re\, H_{22}}{Im\, H_{12} H_{21}} . \qquad (3.14)$$

The surface of P_o in the (L,M,P_o) space is the upward convex paraboloid when $Re\, H_{22} > 0$, and downward convex paraboloid when $Re\, H_{22} < 0$. The P_i and P_o are also represented by means of P_{io}, P_{oo} and χ, where P_{io} and P_{oo} are the input and output power at the point L=1 and M=0, and the positive χ axis extends towards ψ from the point L=1 and M=0. The angle ψ has been given by

$$\psi = \arg (-H_{12} H_{21})^* , \qquad (3.15)$$

which is the angle between the L axis and the image line of gradient line of P_i plane on the LM plane. ψ is caused by the phase rotation between the input and output of a two-port and is reduced to zero for the unilateral two-port. The P_i plane intersects the

x axis in the region of $|\chi| \leq 1$ if $|K| \geq 1$, and in the region of $|\chi| > 1$ if $|K| < 1$, where K has been given by

$$K = \frac{\pm |H_{12} H_{21}|}{2 \operatorname{Re} H_{11} \operatorname{Re} H_{22} - \operatorname{Re} H_{12} H_{21}} . \qquad (3.16)$$

The plus sign corresponds to $\operatorname{Re} H_{22} > 0$, and the minus sign to $\operatorname{Re} H_{22} < 0$. K is a specific quantity in each two-port and contributes to the stability of a two-port. K is reduced to zero for an unilateral two-port. F_o has a positive value when either $|\chi| < 1$ and $\operatorname{Re} H_{22} > 0$, or $|\chi| > 1$ and $\operatorname{Re} H_{22} < 0$.

The ratio of the input and output power at L=1, M=0 has been given by

$$\frac{P_{oo}}{P_{io}} = \frac{|H_{21}|^2}{4 \operatorname{Re} H_{11} \operatorname{Re} H_{22} - 2 \operatorname{Re} H_{12} H_{21}} . \qquad (3.17)$$

The power gain given by Eq. 3.17 is realized by using the load admittance equal to H_{22}^*. For the unilateral two-port ($H_{12}=0$), it represents a unilateral power gain under the complex conjugate matching (i.e. $Z_S = H_{11}^*$, $Y_L = H_{22}^*$). When $1 > K > 0$, the difference between F_{oo}/F_{io} and the complex conjugate matching power gain matched both at the input and the output

is known not to be greater than 3 db.

The values of ψ, K and P_{oo}/P_{io} described here are determined only by the operating condition of given linear active two-port, characterize the nature of the two-port and can be used as the figure of merit of the two-port. The set of these values plays an important role on the design method of high frequency transistor amplifiers in a later section.

The input and load immittances can be expressed in terms of L and M defined in Fig. 3.3. Z_{in} for specific values of L and M can be obtained from the input impedance overlay of Linvill which is a rectangular grid inside the circle with the radius twice as large as that of Linvill chart. In order to obtain the matching source impedance from the readings of α_s and β_s on the input impedance overlay, the following equation is used,

$$Z_s = H_{11}^* + (\alpha_s - j\beta_s)\frac{|H_{12}H_{21}|}{2\,\mathrm{Re}\,H_{22}} . \qquad (3.18)$$

The relation between the load admittance and L, M leads to

$$\left(L - \frac{\mathrm{Re}\,H_{22}}{\mathrm{Re}\,Y_2}\right)^2 + M^2 = \left(\frac{\mathrm{Re}\,H_{22}}{\mathrm{Re}\,Y_2}\right)^2 \qquad (3.19)$$

and

$$L^2 + \left(M + \frac{Re\, H_{22}}{Im\, Y_2}\right)^2 = \left(\frac{Re\, H_{22}}{Im\, Y_2}\right)^2 , \qquad (3.20)$$

where $Y_2 = Y_L + H_{22}$. The set of loci specified by Eq. 3.19 and 3.20 on the same axis when $G_L Re\, H_{22} > 0$ is called the Linvill chart. Y_2 or Y_L for given L and M, and conversely L and M for specified Y_L can be determined from this chart. The Linvill chart is not defined when $G_L Re\, H_{22} < 0$. When the loci of Eqs. 3.19 and 3.20 are drawn outside the Linvill chart, all the load admittance are represented as shown in Fig. 3.4. The relation between Y_L and the readings α_L and β_L on the extended Linvill chart is given by

$$Y_L = (\alpha_L + j\beta_L)\, Re H_{22} - H_{22} . \qquad (3.21)$$

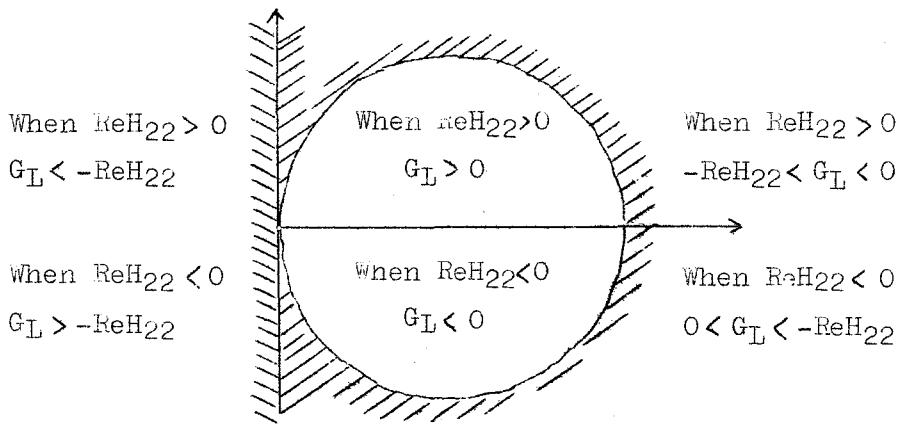

Fig. 3.4 Relation between G_L and extended Linvill chart.

3.4 Power Gain Chart of Linear Active Two-port (38)-(39)

The power gain chart on which the power gain in the stable region of linear active two-port can be obtained graphically for the specified terminations is presented in this section. The power gain is expressed in terms of L and M as

$$G = \frac{P_o}{P_i} = \frac{-(L^2+M^2)|H_{21}|^2 + 2L|H_{21}|^2}{4\,\mathrm{Re}H_{11}\,\mathrm{Re}H_{22} - 2L\,\mathrm{Re}H_{12}H_{21} + 2M\,\mathrm{Im}H_{12}H_{21}} \quad (3.22)$$

It follows that

$$\left(L-1-G\frac{\mathrm{Re}H_{12}H_{21}}{|H_{21}|^2}\right)^2 + \left(M+G\frac{\mathrm{Im}H_{12}H_{21}}{|H_{21}|^2}\right)^2 = \frac{G^2|H_{12}|^2 - 2G(2\mathrm{Re}H_{11}\mathrm{Re}H_{22} - \mathrm{Re}H_{12}H_{21}) + |H_{21}|^2}{|H_{21}|^2} \quad (3.23)$$

assuming G being constant. When the right hand side of Eq. 3.23 is positive, the locus of Eq. 3.23 shows the family of circles for constant G on the LM plane, where

radii; $$\frac{\sqrt{G^2|H_{12}|^2 - 2G(2\mathrm{Re}H_{11}\mathrm{Re}H_{22} - \mathrm{Re}H_{12}H_{21}) + |H_{21}|^2}}{|H_{21}|} \quad (3.24)$$

centers;
$$L = 1 + G\frac{\mathrm{Re}H_{12}H_{21}}{|H_{21}|^2} \quad (3.25)$$

$$M = -G\frac{\mathrm{Im}H_{12}H_{21}}{|H_{21}|^2} \quad (3.26)$$

The locus of centers as G varies is given by

$$M = -(L-1)\frac{\mathrm{Im}\, H_{12} H_{21}}{\mathrm{Re}\, H_{12} H_{21}} \quad , \tag{3.27}$$

which is obtained by eliminating G from Eqs. 3.25 and 3.26. The straight line expressed by Eq. 3.27 is orthogonal to that of Eq. 3.14 and is parallel to the image line of gradient line of P_i on the LM plane.

The range of G is found from the condition that the right hand side of Eq. 3.23 is non-negative. Namely,

$G \geq \alpha_2$, $\alpha_1 \geq G$ if $1 > |K|$

G may take on any values if $1 \leq |K|$, ,

where α_1 and α_2 ($\alpha_2 > \alpha_1$) are the solutions of the equation which is obtained by making the right hand side of Eq. 3.23 zero, that is,

$$\left.\begin{matrix}\alpha_2 \\ \alpha_1\end{matrix}\right\} = \frac{2\mathrm{Re}H_{11}\mathrm{Re}H_{22} - \mathrm{Re}H_{12}H_{21} \pm \sqrt{(2\mathrm{Re}H_{11}\mathrm{Re}H_{22} - \mathrm{Re}H_{12}H_{21})^2 - |H_{12}H_{21}|^2}}{|H_{12}|^2} \quad . \tag{3.28}$$

These values are the power gain under the condition of complex conjugate matching at the input and output. It also can be shown that they are the eigenvalues of characteristic gain matrix which is defined in Section 5.2.

On the other hand, power gain is represented as the function of x

$$G = \frac{P_{oo}}{P_{io}} \cdot \frac{1-x^2}{1+Kx} \equiv \frac{P_{oo}}{P_{io}} G_N \cdot \tag{3.29}$$

The curves of G_N for $|x| \leq 1$, are shown in Fig. 3.5 and 3.6. If $1 > |K|$, G in Eq. 3.29 has the stationary values which coincide with α_1 and α_2 . From Eq. 3.29 we have

$$x^2 + K G_N x + G_N - 1 = 0 \cdot \tag{3.30}$$

Solving this equation with respect to G_N under the condition that Eq. 3.30 has only one solution, we get the stationary values of G_N when $1 > |K|$. Therefore, Eq. 3.30 has no real solution between the two stationary values. This means that there is no real G between the two stationary values. This result agrees with the previously obtained range for G. If $|K| \geq 1$, Eq. 3.30 has real solutions γ and δ ($\gamma \geq \delta$), where

$$\left.\begin{aligned} \gamma + \delta &= -K G_N \\ \gamma \delta &= G_N - 1 \end{aligned}\right\} \cdot \tag{3.31}$$

The circles for constant G_N instersect the x axis at γ and δ when $|K| \geq 1$ and are represented by

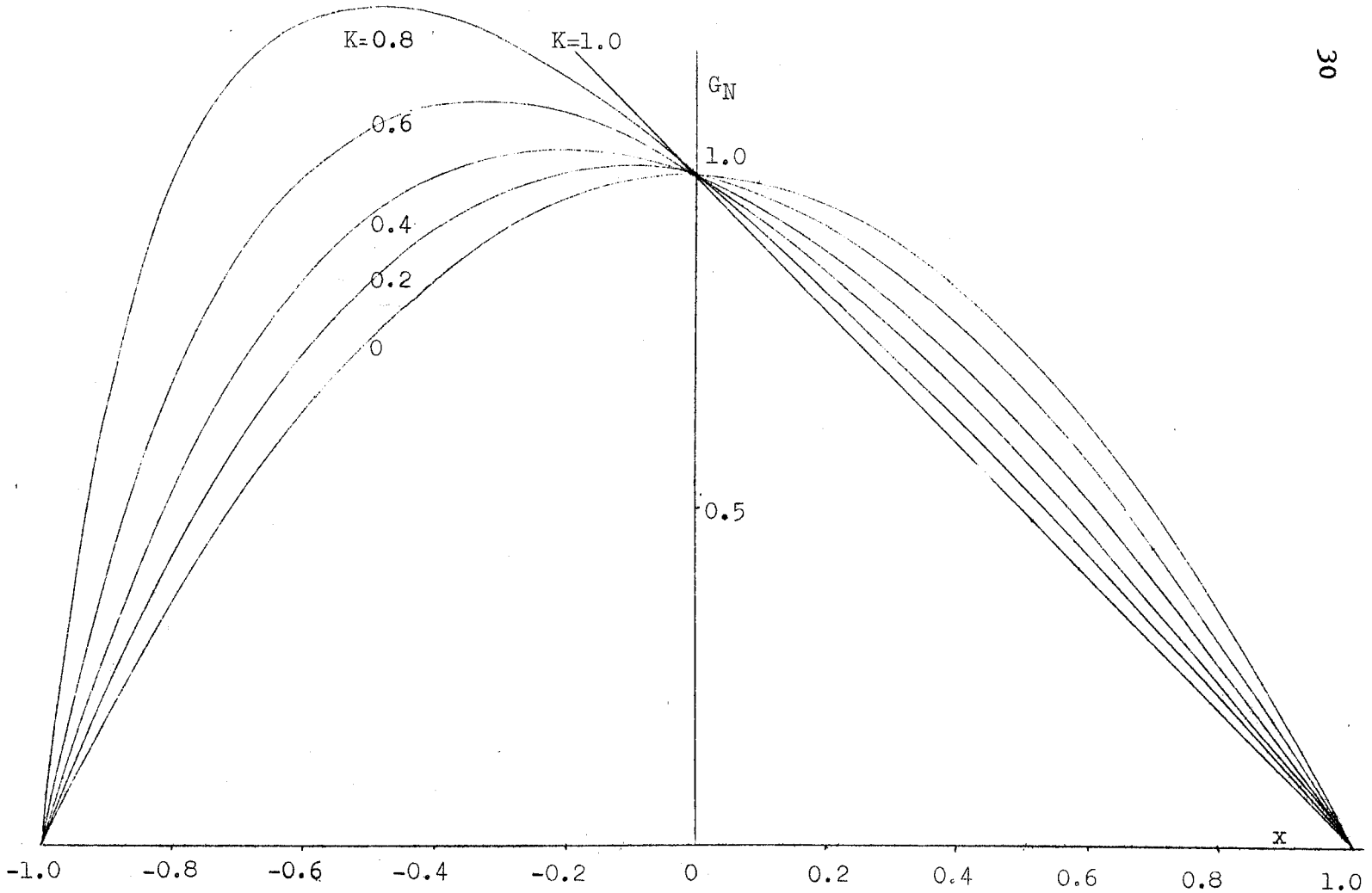

Fig. 3.5 Curves of G_N with parameter K for $1 \geq K \geq 0$, when $|x| \leq 1$.

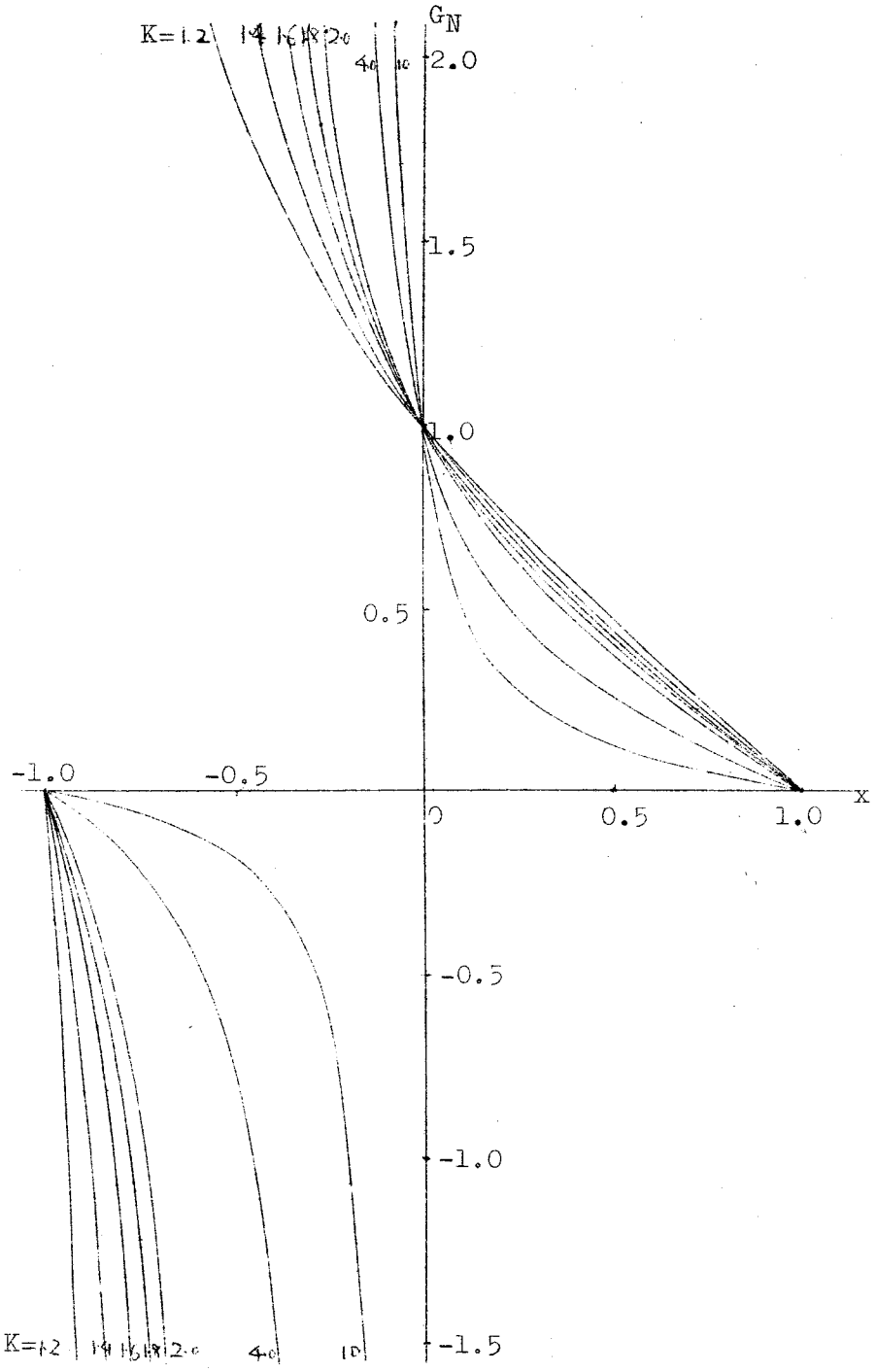

Fig. 3.6 Curves of G_N with parameter K for $K > 1$, when $|x| \leq 1$.

$$\left(x - \frac{\gamma+\delta}{2}\right)^2 + y^2 = \left(\frac{\gamma-\delta}{2}\right)^2 , \qquad (3.32)$$

where the y axis intersects with the x axis orthogonally at the point of L=1 and M=0 in the LM plane. The straight line which intersects the cross points of Eq. 3.32 with the unit circle of $x^2+y^2=1$ is described by

$$\chi = -\frac{1}{K} . \qquad (3.33)$$

Therefore, the family of circles for constant G_N intersect with the unit circle at $\chi = \frac{-1}{K}$ if $|K| > 1$.

Through these considerations, we can draw a family of circles for constant power gain. The example of power gain chart for each case is illustrated in Fig. 3.7. Several power gain charts with parameter K which are traced on transparent paper must be prepared for the following design method of high frequency transistor amplifiers.

3.5 A Design Method of High Frequency Transistor Amplifiers[40]

In this section, a graphical design method of high frequency transistor amplifiers is described

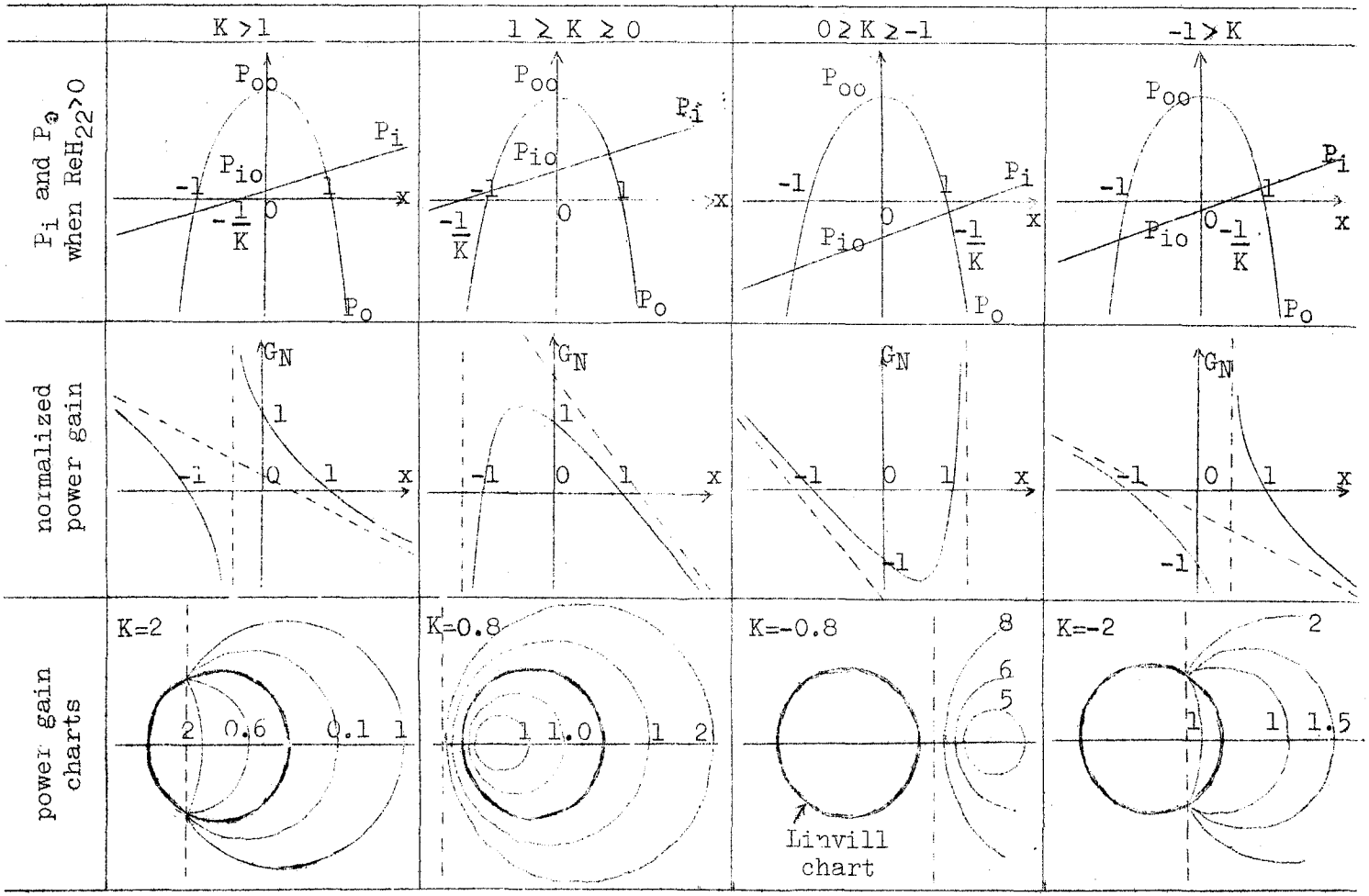

Fig. 3.7 Power gain chart with parameter K.

as an application of the previously mentioned general theory.

(A) Statement of the Problem

The design method deals with the following problems under the condition of complex conjugate matching at the input for an arbitrary load.

(1) The determination of the maximum power gain of an amplifier and its realization. (The maximum power gain does not necessarily require the complex conjugate matching at the input and output of a two-port.)

(2) The determination of power gain of an amplifier with a specified source impedance (or load admittance) and its realization.

(3) The realization of specified power gain below the maximum power gain.

(4) The synthesis with real Z_S for the maximum power gain.

(5) The synthesis with real Y_L for the maximum power gain.

(6) The estimation of the expected variation of the power gain due to the parameter change caused by the change of external circumstances (bias, tempera-

ture, frequency, etc.).

(7) The stability of a given linear active two-port.

(B) Design Method

The design procedures of high frequency transistor amplifiers for $ReH_{22}>0$ using the Linvill chart, the input impedance overlay and the power gain chart, and Eqs. 3.15, 3.16, 3.17, 3.18 and 3.21 are as follows.

1) Measure the H parameter (or other parameter) of the transistor at the desired frequency under a given condition and compute ψ, K and P_{oo}/P_{io} from Eqs. 3.15, 3.16 and 3.17.

2) Determine the power gain chart to be used according to K computed in procedure 1). (If $0>K>-1$, a stable amplifier can not be designed.)

3) Place the power gain chart which has been determined in procedure 2) over the Linvill chart and place the input impedance overlay over them so that the point of Linvill chart corresponding to the infinite reading is at the center of input impedance overlay, and rotate counterclockwise by the angle

both the power gain chart and the input impedance overlay.

In the following the procedures are described in sequence for the above mentioned each problem.

For problem (1)

4) Compute the maximum power gain by substituting the maximum reading G_N which is obtained from the power gain chart into

$$G(db) = \frac{P_{oo}}{P_{io}}(db) + G_N(db) \qquad (3.34)$$

For $1 > K > 0$, G_N is below 3 db. Compute Z_S by substituting the readings α_S and β_S which are obtained on the input impedance overlay at the maximum point of G_N into Eq. 3.18. Then compute Y_L by substituting the readings α_L and β_L which are obtained on the Linvill chart at the maximum point into Eq. 3.21,

For problem (2)

5) As an operating point on the input impedance overlay can be determined from the computed values of α_S and β_S by Eq. 3.18 for the specified source impedance, compute the power gain and the load admittance to be connected with by substituting the readings G_N

on the power gain chart and α_L , β_L on the Linvill chart at this operating point into Eqs. 3.34 and 3.21. As an operating point on the Linvill chart can be determined from the computed values of α_L and β_L by Eq. 3.21 for the specified load admittance, compute the power gain and the source impedance to be connected with by substituting the readings G_N on the power gain chart and α_S , β_S on the input impedance overlay at this operating point into Eqs. 3.34 and 3.18.

For problem (3)

6) If a power gain less than its maximum of the two-port is specified, compute G_N from Eq. 3.34, then a circle on the power gain chart can be specified. Determine the source impedance and the load admittance to realize the specified power gain by substituting the arbitrary readings of α_S , β_S in the input impedance overlay and α_L , β_L in the Linvill chart on the above circle into Eqs. 3.18 and 3.21. The source impedance and the load admittance here cannot be determined uniquely.

For problem (4)

7) Select a line for specified β_S from Eq. 3.18 for $X_S = 0$ on the input impedance overlay and find out a circle which is tangent to (if $|K| > 1$, intersects) this line on the power gain chart. Then compute the maximum power gain for this case by substituting the reading G_N on the power gain chart at the contact (cross) point into Eq. 3.34. If $|K| > 1$, G_N becomes fairly large. Then compute R_S and the load admittance by substituting the readings α_S on the input impedance overlay and α_L, β_L on the Linvill chart at this point into Eqs. 3.18 and 3.21.

For problem (5)

8) Select an arc of the circle for specified β_L from Eq. 3.21 for $B_L = 0$ on the Linvill chart and find out a circle which is tangent to (if $|K| > 1$, may intersect) this arc of the circle on the power gain chart. Then compute the maximum power gain for this case by substituting the reading G_N on the power gain chart at the contact (cross) point into Eq. 3.34. If $|K| > 1$, G_N may become fairly large. Compute the source impedance and G_L by substituting the readings

α_S , β_S on the input impedance overlay and α_L on the Linvill chart at this point into Eqs. 3.18 and 3.21.

For problem (6)

9) If the circumference conditions are varied after the design of transistor amplifier, α_S , β_S , α_L , β_L , Ψ , K and P_{oo}/P_{io} may vary due to the change of H parameters. The difference between the actual power gain and the designed value can be evaluated from the readings of new operating point on the power gain chart.

For problem (7)

10) In Fig. 3.3 the normal power flows are from the source to the two-port and from the two-port to the load, and it can be easily understood that the power flow from the load to the two-port or from the two-port to the source means the unstability of an amplifier. The ranges in which a stable amplifier can be designed lie inside the Linvill chart if $ReH_{22} > 0$ and outside the Linvill chart if $ReH_{22} < 0$. So $G_L > 0$ is necessary to design a stable amplifier. There is no restriction on B_L . The stable region of a two-

port required by the positive input power have been described in the power gain chart. The source impedance of the stable amplifier must be represented in a part of input impedance overlay which is covered with the stable region of power gain chart. This gives the restrictions to the realizability of procedures 5), 7) and 8).

Summarizing the above;

When $1 \geq K \geq 0$, we can design a stable transistor amplifier only in the Linvill chart. Note that, when K=0, that is, when the two-port is unilatural, $ReH_{11} > 0$ is required.

When $0 > K \geq -1$, it is impossible to design a stable amplifier with this transistor because the output power or the input power is always negative.

When $|K| > 1$, this transistor is potentially unstable, which means that a stable amplifier can be designed with this transistor only by the use of suitable terminations. In addition, a fairly high power gain can be expected near the critical points, but it must be remembered that the amplifier may become unstable by the variation of external condi-

tion.

For the transistor of $ReH_{22} < 0$, the range of positive output power is outside the Linvill chart. But the proposed design method in this case is effective by using the extended Linvill chart and the power gain chart outside the Linvill chart as illustrated in Fig. 3.7.

3.6 Determination of Bandwidth on Family of Circles for Constant Power Transfer Ratio[41]

The discussion on bandwidth of high frequency transistor amplifiers using the power transfer ratio is described in this section. It is well known that the complex conjugate matching is used in order to obtain the high gain. The relation between the departure from matching and the decrease of power gain, and the determination method of bandwidth using the power transfer ratio are clarified.

The power transfer ratios T_{in} , T_{out} at the input and the output of an amplifier are represented by

$$T_{in} = \frac{\text{Input power}}{\text{Exchangeable power of source}} = \frac{4R_S R_{in}}{|Z_S + Z_{in}|^2} \qquad (3.35)$$

$$T_{out} = \frac{\text{Power to load}}{\text{Exchangeable power of output}} = \frac{4G_{out}G_L}{|Y_{out}+Y_L|^2} \quad (3.36)$$

The power transfer ratio is unity if all the available power of the source flows into the load. In this case the available power of source is consumed in the source and the load respectively. $T_{in}=1$ means the input matching and $T_{out}=1$ means the output matching. The problem (1) in preceding section is concerned with the realization method of $T_{in}=T_{out}=1$, and the problem (2) is that of $T_{in}=1$ and $T_{out}\neq 1$.

In order to estimate the mismatching effect at the input and output, from Eqs. 3.35 and 3.36 making T_{in} and T_{out} be constants, following equations are led

$$\left\{R_{in}+R_S\left(1-\frac{2}{T_{in}}\right)\right\}^2+(X_{in}+X_S)^2=\frac{4R_S^2(1-T_{in})}{T_{in}^2} \quad (3.37)$$

$$\left\{R_S+R_{in}\left(1-\frac{2}{T_{in}}\right)\right\}^2+(X_S+X_{in})^2=\frac{4R_{in}^2(1-T_{in})}{T_{in}^2} \quad (3.38)$$

$$\left\{G_L+G_{out}\left(1-\frac{2}{T_{out}}\right)\right\}^2+(B_L+B_{out})^2=\frac{4G_{out}^2(1-T_{out})}{T_{out}^2} \quad (3.39)$$

$$\left\{G_{out}+G_L\left(1-\frac{2}{T_{out}}\right)\right\}^2+(B_{out}+B_L)^2=\frac{4G_L^2(1-T_{out})}{T_{out}^2}. \quad (3.40)$$

The loci of these equations form the families of circles for constant T_{in} and T_{out} if Z_S, Z_{in}, Y_{out} and Y_L are constants inside of the necessary bandwidth. The mismatching effect at the input and output side of the input tuned amplifier, in which Z_{in} and Y_L are nearly constant, can be estimated by Eqs. 3.38 and 3.40 respectively. In case of the output tuned amplifier, in which Z_S and Y_{out} are nearly constant, the mismatching effect at the input and output side can be estimated by Eqs. 3.37 and 3.39. Usually Eqs. 3.38 and 3.39 are more effective in those estimations. For example, in case of the output tuned amplifier of $T_{in} = T_{out}=1$ at center frequency, after drawing the circle of $T_{out} = \frac{1}{2}$ by Eq. 3.39 on the load admittance plane and ploting the load admittance including the tuned circuit on the same scale, we can determine the bandwidth between the points corresponding to -3db by the frequency at which the load admittance intersects the circle of $T_{out} = \frac{1}{2}$. The family of cirles for constant power transfer ratio of output tuned transistor amplifiers and its cross section is illustrated in Fig. 3.8.

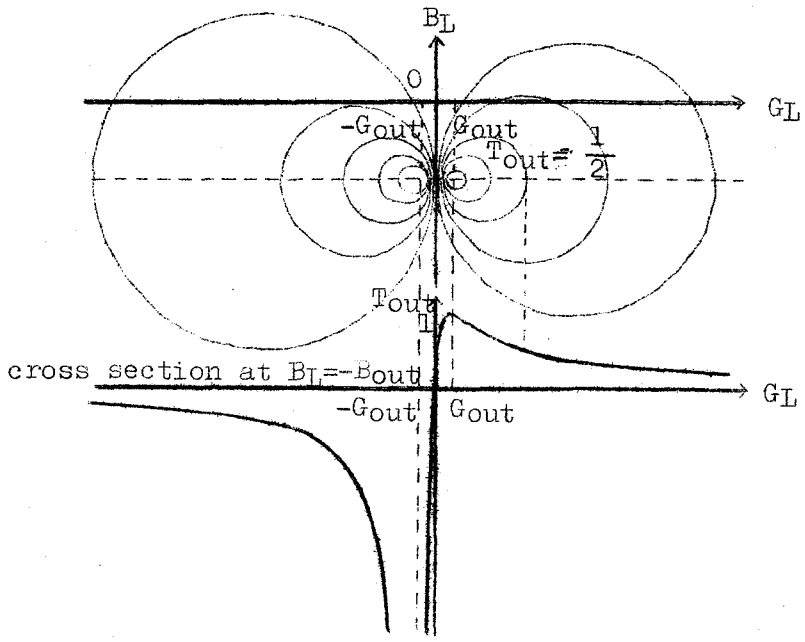

Fig. 3.8 Family of circles for constant power transfer ratio of output tuned transistor amplifiers and its cross section.

3.7 Designing Illustrations of High Frequency Transistor Amplifiers[35],[41],[42]

The experimental results by the previous mentioned design method are described in this section and the justification of this method is clarified. The transistor used is 2SA235. H parameters and other immittances are measured by the Transfer and Immittance Function Meter of General Radio (TIF meter).

As the difference of readings on the power gain chart

due to the slight change of ψ, K is not significant, the design method may be easily applied to the transistor. Figures 3.9 and 3.10 show the curves of ψ, K, P_{oo}/P_{io} and α_1, calculated from the H parameters, as dependent on collector current. As the collector current characteristics of ψ and K for both grounding methods show only a slight change, this design method may be applied conveniently. The same argument also applies to the collector voltage characteristics, as can be seen in Fig. 3.11 and 3.12. As K of this transistor is between unity and zero, the stable amplifier can be designed always according to this design method by using the terminations inside the Linvill chart ($G_L > 0$, because $ReH_{22} > 0$). It is also shown that the difference between the maximum power gain α_1 and P_{oo}/P_{io} is less than 3db. The grounded base configuration is desirable than the grounded emitter configuration in designing amplifier judging from the collector current characteristics of α_1. The collector voltage characteristics of P_{oo}/P_{io} for both grounding methods are flat, as can be seen in Fig. 3.13. The collector current characteristics of terminating impedances which

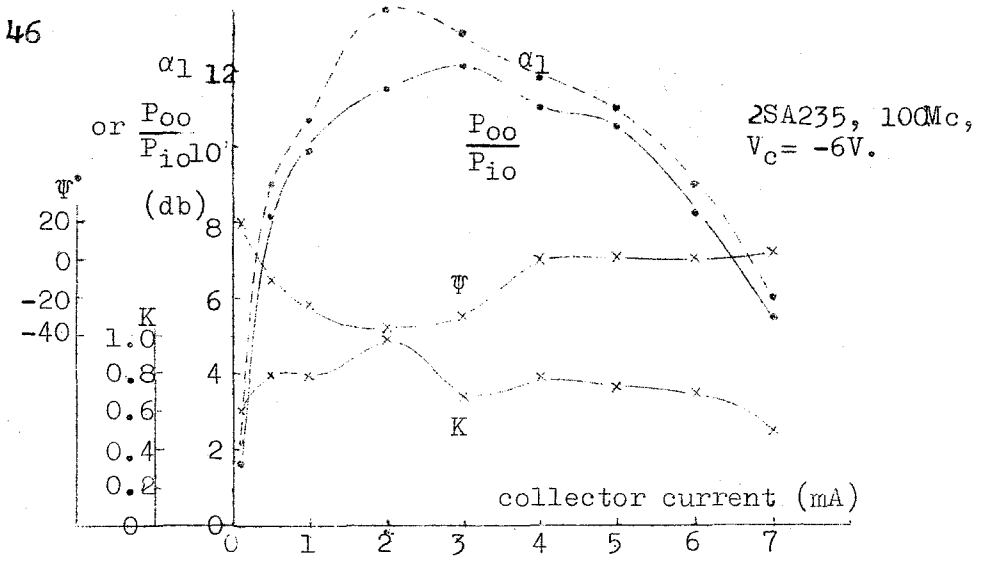

Fig. 9 Curves of Ψ , K, P_{oo}/P_{io} and α_1 , calculated from the H parameters in grounded base configuration, as dependent on collector current.

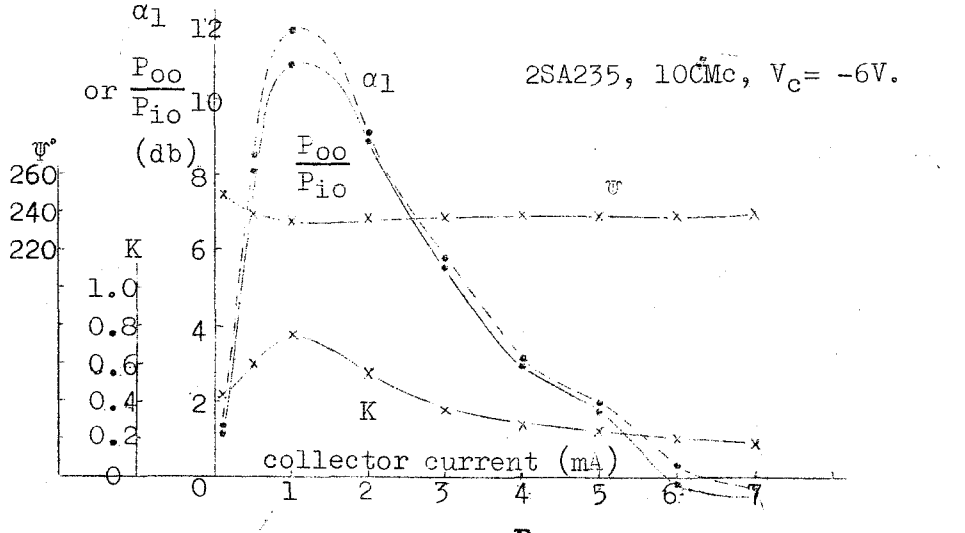

Fig. 10 Curves of Ψ , K, P_{oo}/P_{io} and α_1 , calculated from the H parameters in grounded emitter configuration, as dependent on collector current.

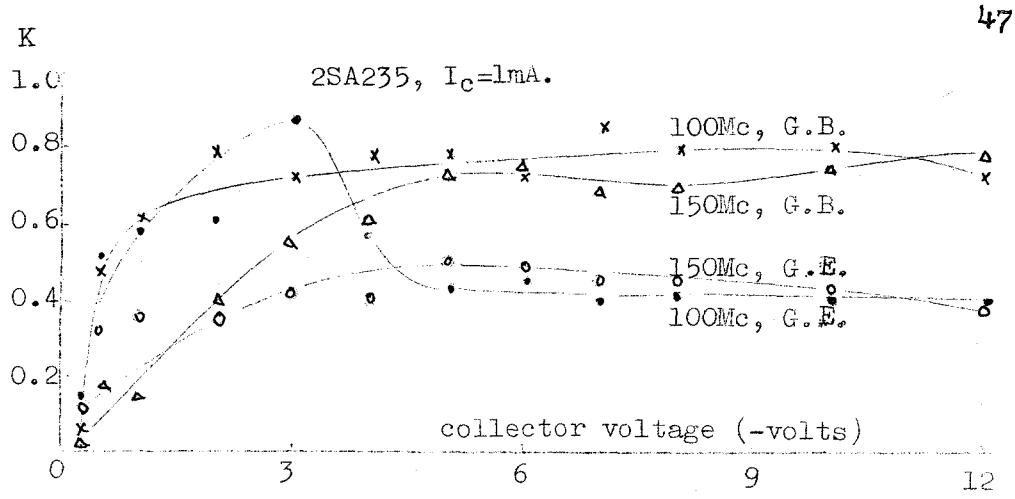

Fig. 3.11 Curves of K as dependent on collector voltage.

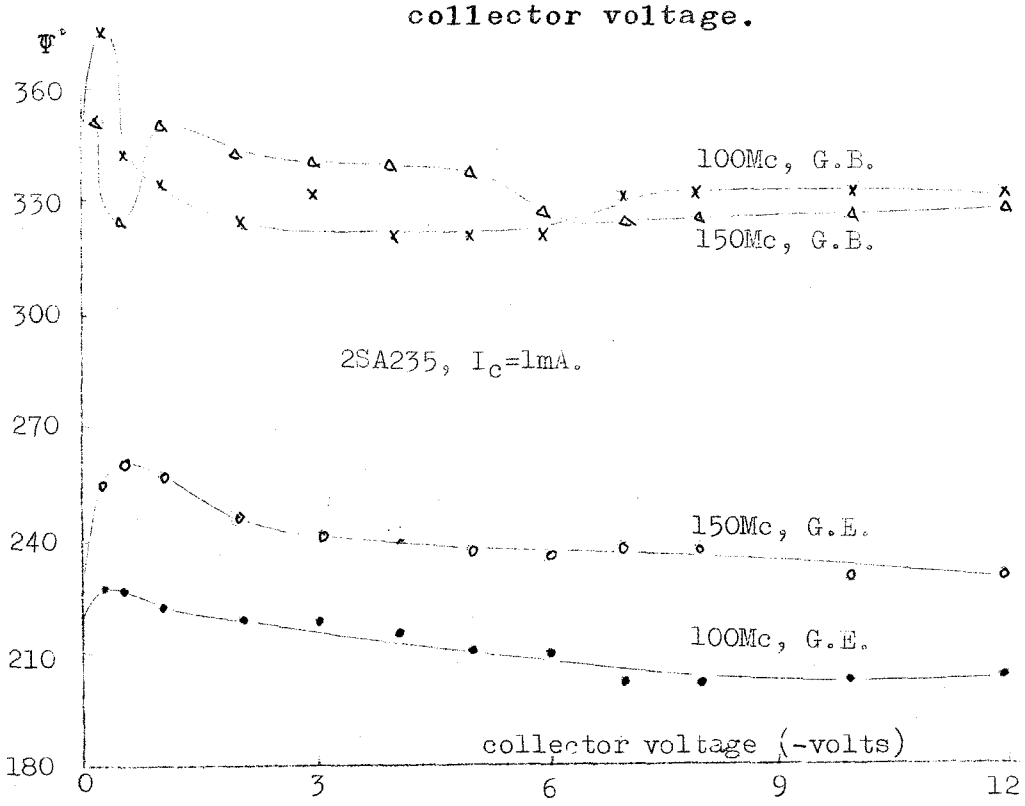

Fig. 3.12 Curves of ψ as dependent on collector voltage.

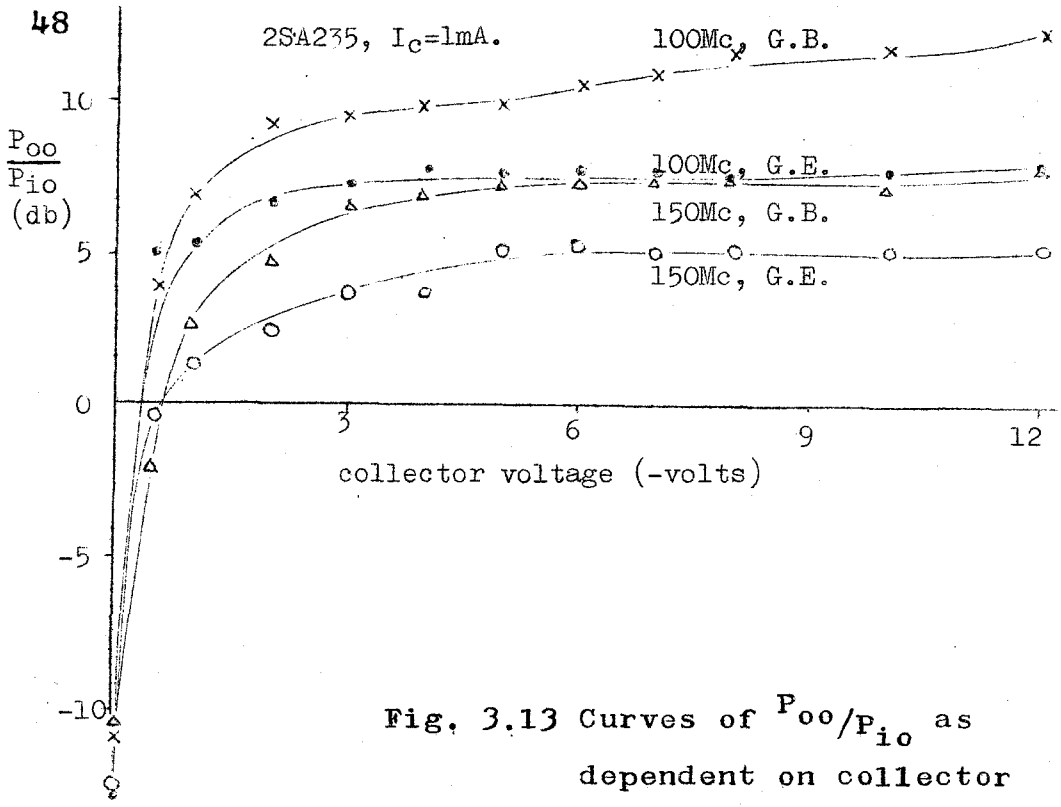

Fig. 3.13 Curves of P_{oo}/P_{io} as dependent on collector voltage.

realize the complex conjugate matching power gain at the input and the output are shown in Figs. 3.14 and 3.15 comparing with those of Z_{11}^* and Z_{22}^*. The complex conjugate matching is nearly obtained by using Z_{11}^*, Z_{12}^* instead of Z_S, Z_L in these figures. This is easily understood from the fact that the termination of Z_{22}^* means the realization of P_{oo}/P_{io} in this design method. In addition, though the

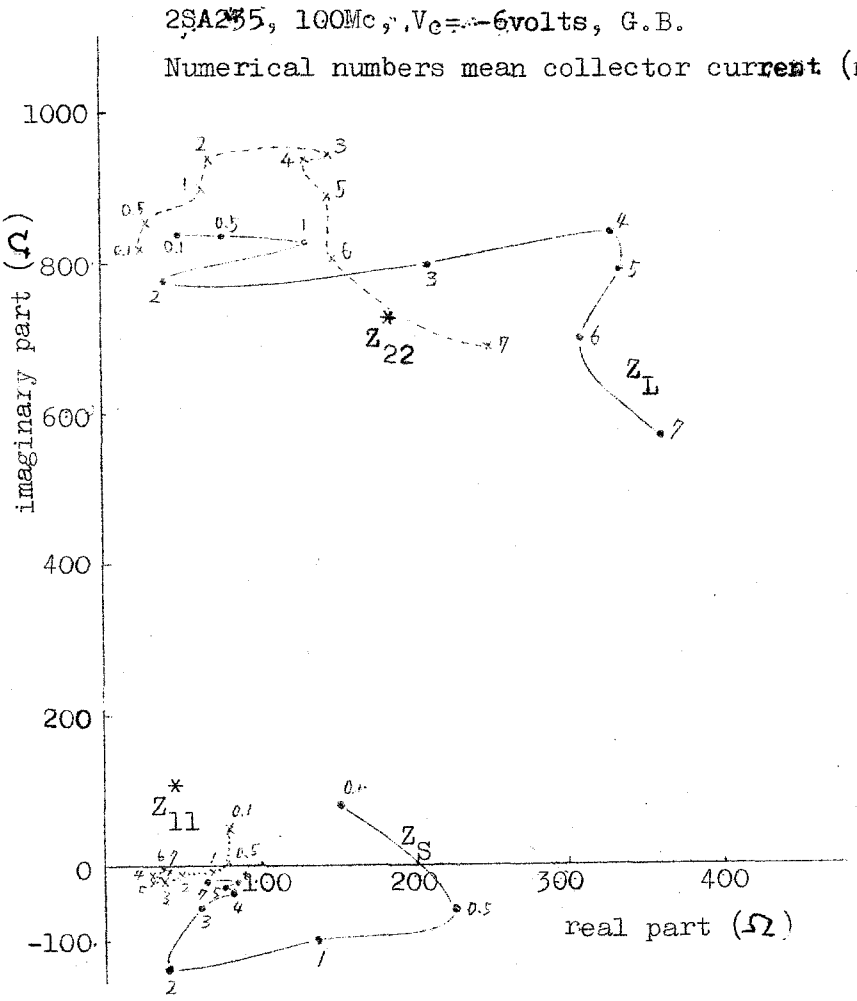

Fig. 3.14 Terminating impedances to realize the complex conjugate matching and Z_{11}^* , Z_{22}^* calculated from the H parameters in grounded base configuration.

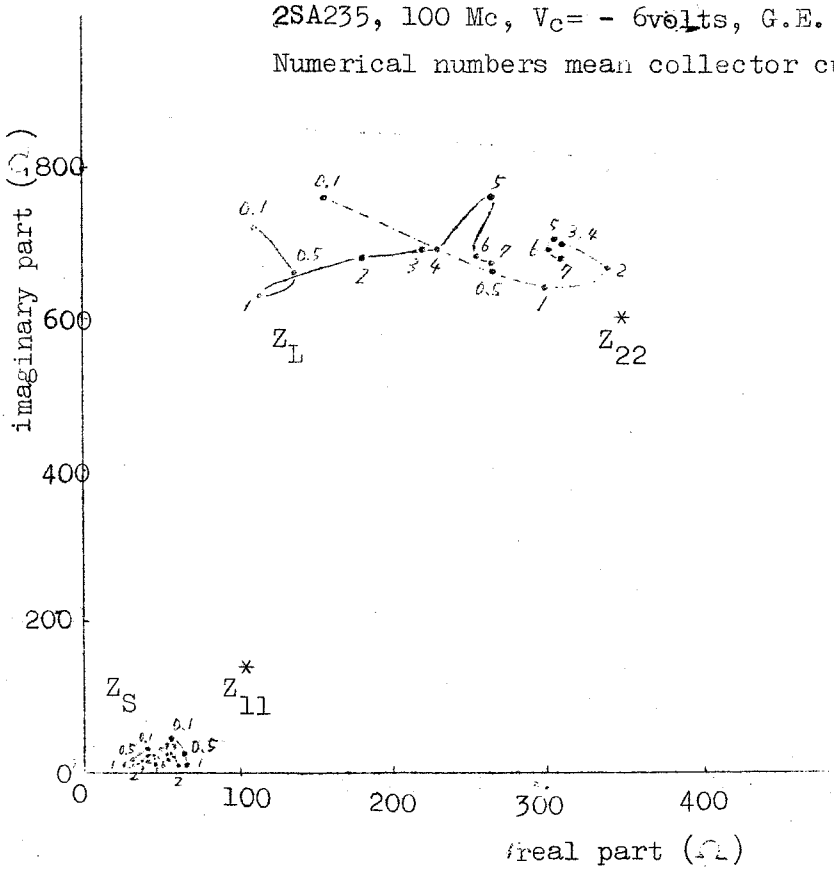

Fig. 3.15 Terminating impedances to realize the complex conjugate matching and Z_{11}^* , Z_{22}^* calculated from the H parameters in grounded emitter configuration.

terminating impedances to realize the complex conjugate matching at the input and the output are obtained by the procedure 4) in Section 3.5, they may be also obtained from Eqs. 5.26 and 5.31.

Now, the problem (2) of Section 3.5 is treated. The illustration of amplifier of the input matching for the specified load impedance $Z_L=840+j420(\Omega)$ is shown in Fig. 3.16. As the source impedance to realize the input matching has the collector current characteristics due to that of input impedance, the source impedances are adjusted for each collector current to satisfy the input matching condition as shown in Fig. 3.17. These data are not the collector current characteristics of an amplifier designed at certain collector current, but is the results of amplifier designed at each collector current independently. The measured values of Fig. 3.16 are in accord with the designed values in each point and the justification of this design method is verified. In addition, the power gain of amplifier designed at certain collector current coincides with the designed value only at the designed point, and it usually decreases from the designed value at another collector

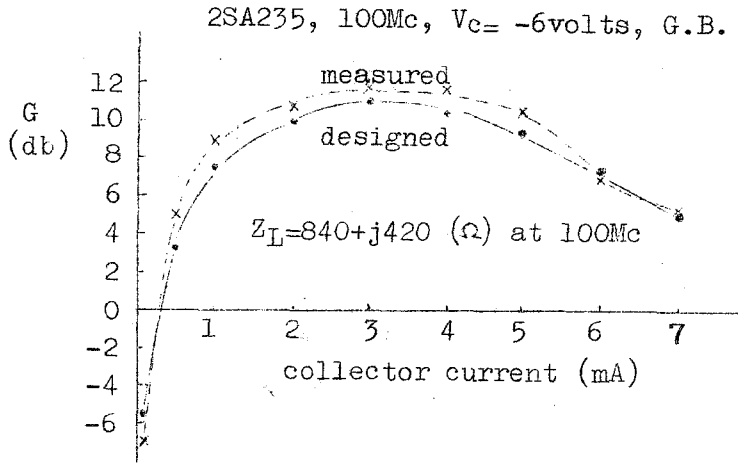

Fig. 3.16 Power gain of input matching amplifiers for a specified load impedance, as indicated, measured in grounded base configuration.

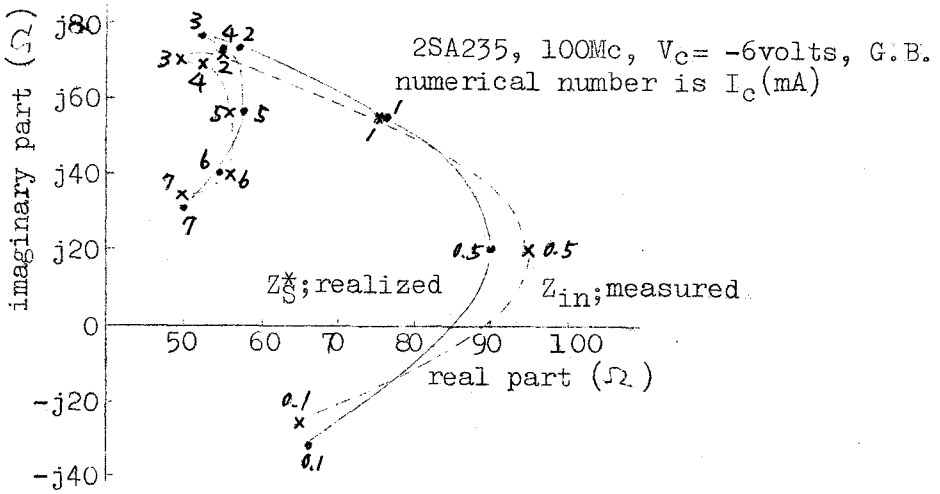

Fig. 3.17 Source impedances and input impedances of the amplifier of Fig.3.16, which realize the input matching.

current due to the mismatching effect at input side. However, this mismatching effect is not so significant and the collector current characteristics of power gain nearly coincides with that of the designed values as can be seen from the collector current characteristics of input impedance and the family of circles for the constant power transfer ratio of Eq. 3.37.

The frequency characteristics of the designed and measured values of the output tuned transistor amplifier are shown in Fig. 3.18. The designed values are obtained for each point after drawing the frequency characteristics of load admittance on the Linvill chart. The measured values of Fig. 3.18 are obtained after the adjustment of source impedance to satisfy the input matching condition for each frequency. There is no trouble if the source impedance with the frequency characteristics specified from that of input impedance is easily realized. The power gain of amplifier which is designed to be matched on the center frequency of the bandwidth at the input side coincides with the designed value only at the center frequency and it usually decrease

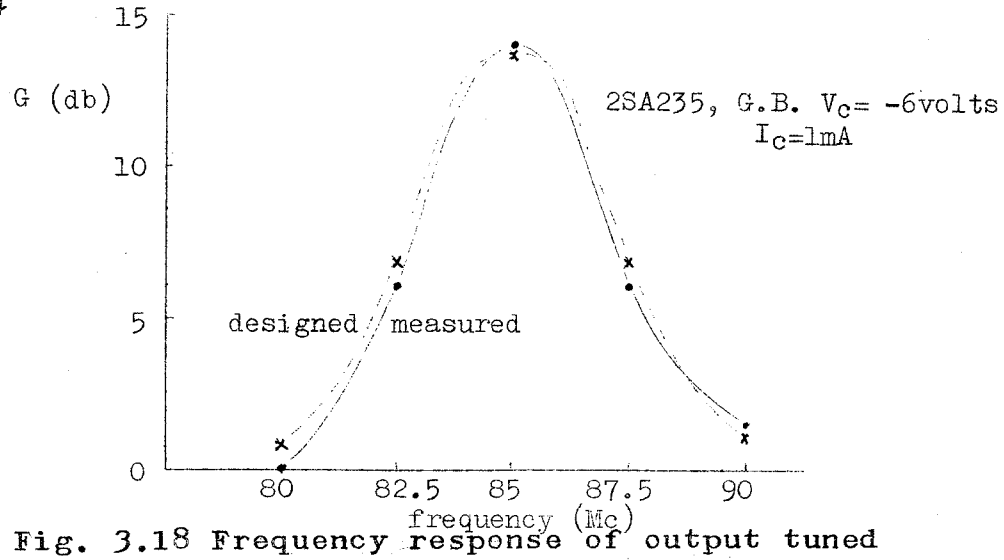

Fig. 3.18 Frequency response of output tuned transistor amplifier.

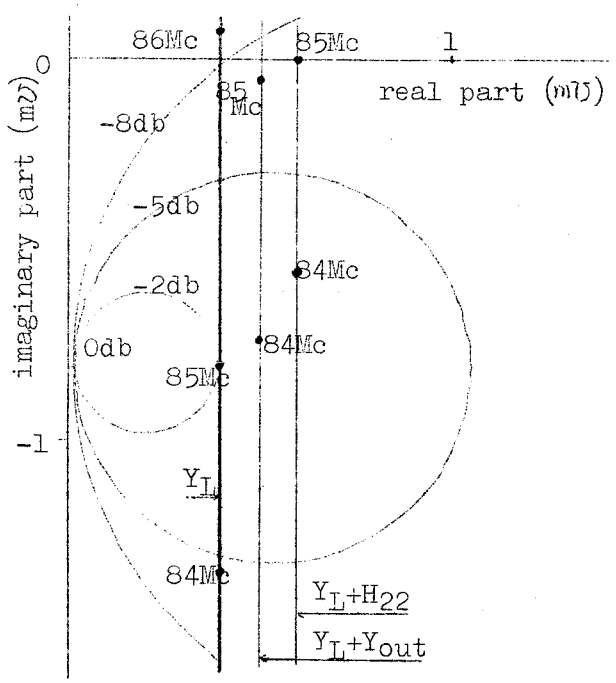

Fig. 3.19 The load admittance of the amplifier of Fig. 3.18 and the circles of constant power transfer ratio.

from the designed value for other frequency due to the mismatching effect at the input side. However, the mismatching effect is not so significant and the frequency characteristics of power gain is nearly agreed with that of designed values as can be also seen from the frequency characteristics of input impedance and that of specified source impedance for which the input matching is obtained at certain frequency. Actually, the frequency characteristics of power gain which is expected from the design method will be almost realized by matching the source impedance which is determined from the antenna and its coupling circuit to the input impedance. The bandwidth of this amplifier is also determined easily from the circles of Eq. 3.39. The load admittance Y_L, (Y_L+H_{22}) and (Y_L+Y_{out}) corresponding to the amplifier of Fig. 3.18 are shown in Fig. 3.19, together with the circle of constant power transfer ratio. At the center frequency (85Mc) the power transfer ratio is -2db. Therefore, the frequency which the curve of Y_L intersects the circle of -5db corresponds to the bandwidth of -3db. If the real part of Y_L is decreased until the Y_L passes the point of 0db, the power gain of 2db is

increased at the center frequency, but the bandwidth may be narrowed relatively.

Usually, the following stage of high frequency amplifiers is the frequency converter. The power gain G' (the ratio of input power of converter to that of amplifier) in this case is given by

$$G' = G \frac{1}{1 + \frac{\mathrm{Re}\, Y_t}{\mathrm{Re}\, Y_c}} , \qquad (3.41)$$

where Y_t is the admittance of the tuned circuit and Y_c is the sum of admittance of the coupling circuit and the input admittance of converter. G is the power gain which is obtained from this design method. Equation 3.41 means that the total power gain decreases due to the loss of the tuned circuit.

3.8 Summary of Chapter III

The power gain chart which indicates the power gain and stability of a linear amplifier for the specified terminations under the condition of the input matching is obtained as a results of general analysis of a linear active two-port using the circuit parameters. A graphical design method of high frequency transistor amplifiers using three kinds of

charts including the power gain chart is reported here as the alternative to the usual method which suffers from the complex computations. Moreover, the mismatching effect is estimated on the charts for constant power transfer ratios and is also used for the determination of the bandwidth of the tuned amplifiers. By this method, the circuit designer is able to design the transistor amplifiers graphically without the considerations of the inside of an active two-port. Finally, the graphical design method is confiimed with the experimental results.

CHAPTER IV NOISY COMPONENTS OF LINEAR ACTIVE TWO-PORT[43]

4.1 Preface

The terminal voltages and currents of linear active two-port are related with each other through circuit parameters. The circuit parameters reveal the performance of a two-port at the absence of internal noise sources. The method of measurement of the circuit parameters have been established and they can be easily measured.

On the other hand, the performance of a two-port at the presence of internal noise sources can be represented completely by the noisefree circuit parameters and the noisy components. It is reported by Rothe and Dahlke[45] that the linear noisy two-port can be divided into noisefree and noisy two-ports, both of which are determined by the operating condition of an active two-port. We have six kinds of representation of noisy components corresponding to each circuit parameter as shown in Fig. 4.1. The relations between the terminal voltages and currents containing the noisy components are expressed

y

$$\begin{pmatrix} V_1 \\ V_2 \end{pmatrix} = \begin{pmatrix} Z_{11} & Z_{12} \\ Z_{21} & Z_{22} \end{pmatrix} \begin{pmatrix} I_1 \\ I_2 \end{pmatrix} + \begin{pmatrix} V_{1Z} \\ V_{2Z} \end{pmatrix} \quad (4.1) \qquad \begin{pmatrix} I_1 \\ I_2 \end{pmatrix} = \begin{pmatrix} Y_{11} & Y_{12} \\ Y_{21} & Y_{22} \end{pmatrix} \begin{pmatrix} V_1 \\ V_2 \end{pmatrix} + \begin{pmatrix} i_{1Y} \\ i_{2Y} \end{pmatrix} \quad (4.2)$$

$$\begin{pmatrix} V_1 \\ I_2 \end{pmatrix} = \begin{pmatrix} H_{11} & H_{12} \\ H_{21} & H_{22} \end{pmatrix} \begin{pmatrix} I_1 \\ V_2 \end{pmatrix} + \begin{pmatrix} V_H \\ i_H \end{pmatrix} \quad (4.3) \qquad \begin{pmatrix} I_1 \\ V_2 \end{pmatrix} = \begin{pmatrix} G_{11} & G_{12} \\ G_{21} & G_{22} \end{pmatrix} \begin{pmatrix} V_1 \\ I_2 \end{pmatrix} + \begin{pmatrix} i_G \\ V_G \end{pmatrix} \quad (4.4)$$

$$\begin{pmatrix} V_1 \\ I_1 \end{pmatrix} = \begin{pmatrix} F_{11} & F_{12} \\ F_{21} & F_{22} \end{pmatrix} \begin{pmatrix} V_2 \\ I_2 \end{pmatrix} + \begin{pmatrix} V_F \\ i_F \end{pmatrix} \quad (4.5) \qquad \begin{pmatrix} V_2 \\ I_2 \end{pmatrix} = \begin{pmatrix} T_{11} & T_{12} \\ T_{21} & T_{22} \end{pmatrix} \begin{pmatrix} V_1 \\ I_1 \end{pmatrix} + \begin{pmatrix} V_T \\ i_T \end{pmatrix} \quad (4.6)$$

here $\overline{v_{1Z}^2}$; square value of input open noise voltage when output is open,

$\overline{v_{2Z}^2}$; square value of output open noise voltage when input is open,

$\overline{i_{1Y}^2}$; square value of input short noise current when output is short,

$\overline{i_{2Y}^2}$; square value of output short noise current when input is short,

$\overline{v_H^2}$; square value of input open noise voltage when output is short,

$\overline{i_H^2}$; square value of output short noise current when input is open,

$\overline{i_G^2}$; square value of input short noise current when output is open,

$\overline{v_G^2}$; square value of output open noise voltage when input is short,

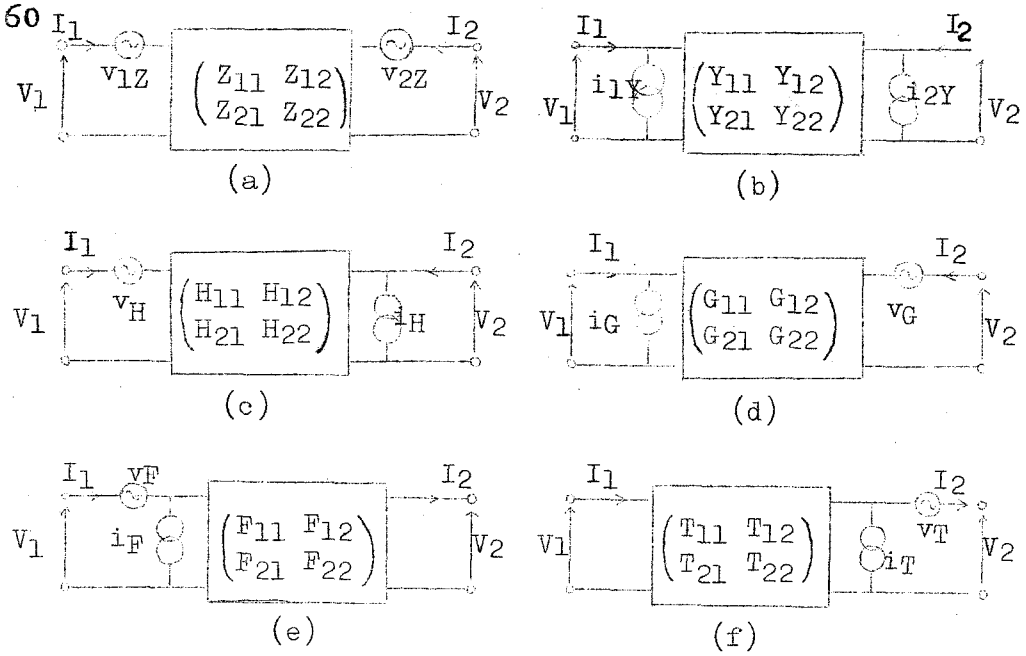

Fig. 4.1 Representations of internal noise sources of linear active two-port in terms of noisy components.

The noisy components of two-port are described by the set of four quantities, that is, two auto-correlation power spectrums, and the real and imaginary parts of crosscorrelation power spectrum. We have transformation formulae between noisy components[46] just as we have the formulae among circuit parameters.

The circuit analysis by means of circuit parameters and noisy components of linear active two-

port is significant on the unified treatment when the two-port has the internal noise sources. Many papers based on this method have been presented. A paper which deals with the measurment of this noisy components, however, has not been reported. Therefore, there is no numerical consideration in such papers as to the measured noisy components. In Chapter IV, the method of measurement for noisy components of two-port is presented and the measured results of a transistor are given.

4,2 Transformation Formulae to Obtain the Set of Noisy Components

The noisy components of linear active two-port are described by four independent quantities, for instance, $\overline{v_F^2}$, $\overline{i_F^2}$ and the complex crosscorrelation spectrum $\overline{v_F i_F^*}$ inF parameter representation, These values are used on the interpretation of noise performance of linear active two-port. The quantities $\overline{i_{1Y}^2}$, $\overline{i_{2Y}^2}$, $\overline{i_H^2}$, $\overline{i_G^2}$ and $\overline{v_{1Z}^2}$, $\overline{v_{2Z}^2}$, $\overline{v_H^2}$, $\overline{v_G^2}$ are measurable directly by the method mentioned in Section 4.3. The quantities $\overline{v_F^2}$, $\overline{i_F^2}$, $\overline{v_T^2}$, $\overline{i_T^2}$ and the

crosscorrelation spectrum of each representation can not be measured directly. In this section, the transformation formulae between such quantities are presented in Table 2. By this formulae we can obtain completely the set of noisy components for each parameter representation. The transformation formulae to obtain the set of noisy components from the noise voltage sources is given from Table 2 using the following equations.

$$\overline{i_{1Y}^2} = |Y_{11}|^2 \overline{V_H^2} \qquad (4.7)$$

$$\overline{i_{2Y}^2} = |Y_{22}|^2 \overline{V_G^2} \qquad (4.8)$$

$$\overline{i_G^2} = |G_{11}|^2 \overline{V_{1E}^2} \qquad (4.9)$$

$$\overline{i_H^2} = |H_{22}|^2 \overline{V_{2E}^2} \qquad (4.10)$$

Table 2 Transformation formulae to obtain the set of noisy components.

	$\overline{V_F^2} = \lvert F_{12}\rvert^2 \overline{i_{2Y}^2}$	$\overline{i_F^2} = \lvert F_{22}\rvert^2 \overline{i_H^2}$
F	$\overline{V_F i_F^*} = \dfrac{\begin{vmatrix} \lvert F_{12}\rvert^2 \overline{i_{2Y}^2} + \lvert Z_{11}\rvert^2 \lvert F_{22}\rvert^2 \overline{i_H^2} - \lvert Z_{11}\rvert^2 \overline{i_G^2} & \mathrm{Im}\, Z_{11} \\ \lvert F_{12}\rvert^2 \overline{i_{2Y}^2} + \lvert F_{12}\rvert^2 \overline{i_H^2} - \lvert H_{11}\rvert^2 \overline{i_{1Y}^2} & \mathrm{Im}\, H_{11} \end{vmatrix} + j \begin{vmatrix} \mathrm{Re}\, Z_{11} & \lvert F_{12}\rvert^2 \overline{i_{2Y}^2} + \lvert Z_{11}\rvert^2 \lvert F_{22}\rvert^2 \overline{i_H^2} - \lvert Z_{11}\rvert^2 \overline{i_G^2} \\ \mathrm{Re}\, H_{11} & \lvert F_{12}\rvert^2 \overline{i_{2Y}^2} + \lvert F_{12}\rvert^2 \overline{i_H^2} - \lvert H_{11}\rvert^2 \overline{i_{1Y}^2} \end{vmatrix}}{2 \begin{vmatrix} \mathrm{Re}\, Z_{11} & \mathrm{Im}\, Z_{11} \\ \mathrm{Re}\, H_{11} & \mathrm{Im}\, H_{11} \end{vmatrix}}$	
	$\overline{V_{1E}^2} = \lvert Z_{11}\rvert^2 \overline{i_G^2}$	$\overline{V_{2E}^2} = \lvert Z_{22}\rvert^2 \overline{i_H^2}$
Z	$\begin{vmatrix} \lvert Z_{12}\rvert^2 \overline{i_H^2} + \lvert Z_{11}\rvert^2 \overline{i_G^2} - \lvert H_{11}\rvert^2 \overline{i_{1Y}^2} & \mathrm{Im}\, H_{12} \\ \lvert Z_{21}\rvert^2 \overline{i_G^2} + \lvert Z_{22}\rvert^2 \overline{i_H^2} - \lvert G_{22}\rvert^2 \overline{i_{2Y}^2} & -\mathrm{Im}\, G_{21} \end{vmatrix}$	

$$\overline{v_{12}\,v_{22}^*} = \frac{+j\begin{vmatrix} \mathrm{Re}\,H_{12} & |Z_{12}|^2\,\overline{i_H^2} + |Z_{11}|^2\,\overline{i_G^2} - |H_{11}|^2\,\overline{i_{1Y}^2} \\ \mathrm{Re}\,G_{21} & |Z_{21}|^2\,\overline{i_G^2} + |Z_{22}|^2\,\overline{i_H^2} - |G_{22}|^2\,\overline{i_{2Y}^2} \end{vmatrix}}{2\begin{vmatrix} \mathrm{Re}\,H_{12} & \mathrm{Im}\,H_{12} \\ \mathrm{Re}\,G_{21} & -\mathrm{Im}\,G_{21} \end{vmatrix}}$$

	$\overline{i_{1Y}^2}$	$\overline{i_{2Y}^2}$
Y	$\overline{i_{1Y}\,i_{2Y}^*} = \dfrac{+j\begin{vmatrix} \overline{i_{2Y}^2} + \lvert H_{21}\rvert^2\,\overline{i_{1Y}^2} - \overline{i_H^2} & -\mathrm{Im}\,H_{21} \\ \overline{i_{1Y}^2} + \lvert G_{12}\rvert^2\,\overline{i_{2Y}^2} - \overline{i_G^2} & \mathrm{Im}\,G_{12} \end{vmatrix}}{2\begin{vmatrix} \mathrm{Re}\,H_{21} & -\mathrm{Im}\,H_{21} \\ \mathrm{Re}\,G_{12} & \mathrm{Im}\,G_{12} \end{vmatrix}}$	$+j\begin{vmatrix} \mathrm{Re}\,H_{21} & \overline{i_{2Y}^2} + \lvert H_{21}\rvert^2\,\overline{i_{1Y}^2} - \overline{i_H^2} \\ \mathrm{Re}\,G_{12} & \overline{i_{1Y}^2} + \lvert G_{12}\rvert^2\,\overline{i_{2Y}^2} - \overline{i_G^2} \end{vmatrix}$
	$\overline{v_H^2} = \lvert H_{11}\rvert^2\,\overline{i_{1Y}^2}$	$\overline{i_H^2}$
H	$\overline{v_H\,i_H^*} = \dfrac{+j\begin{vmatrix} \overline{i_H^2} + \lvert H_{21}\rvert^2\,\overline{i_{1Y}^2} - \overline{i_{2Y}^2} & -\mathrm{Im}\,Y_{21} \\ \lvert Z_{12}\rvert^2\,\overline{i_H^2} + \lvert H_{11}\rvert^2\,\overline{i_{1Y}^2} - \lvert Z_{11}\rvert^2\,\overline{i_G^2} & \mathrm{Im}\,Z_{12} \end{vmatrix}}{2\begin{vmatrix} \mathrm{Re}\,Y_{21} & -\mathrm{Im}\,Y_{21} \\ \mathrm{Re}\,Z_{12} & \mathrm{Im}\,Z_{12} \end{vmatrix}}$	$+j\begin{vmatrix} \mathrm{Re}\,Y_{21} & \overline{i_H^2} + \lvert H_{21}\rvert^2\,\overline{i_{1Y}^2} - \overline{i_{2Y}^2} \\ \mathrm{Re}\,Z_{12} & \lvert Z_{12}\rvert^2\,\overline{i_H^2} + \lvert H_{11}\rvert^2\,\overline{i_{1Y}^2} - \lvert Z_{11}\rvert^2\,\overline{i_G^2} \end{vmatrix}$
	$\overline{i_G^2}$	$\overline{v_G^2} = \lvert G_{22}\rvert^2\,\overline{i_{2Y}^2}$
G	$\overline{i_G\,v_G^*} = \dfrac{+j\begin{vmatrix} \overline{i_G^2} + \lvert G_{12}\rvert^2\,\overline{i_{2Y}^2} - \overline{i_{1Y}^2} & \mathrm{Im}\,Y_{12} \\ \lvert Z_{21}\rvert^2\,\overline{i_G^2} + \lvert G_{22}\rvert^2\,\overline{i_{2Y}^2} - \lvert Z_{22}\rvert^2\,\overline{i_H^2} & -\mathrm{Im}\,Z_{21} \end{vmatrix}}{2\begin{vmatrix} \mathrm{Re}\,Y_{12} & \mathrm{Im}\,Y_{12} \\ \mathrm{Re}\,Z_{21} & -\mathrm{Im}\,Z_{21} \end{vmatrix}}$	$+j\begin{vmatrix} \mathrm{Re}\,Y_{12} & \overline{i_G^2} + \lvert G_{12}\rvert^2\,\overline{i_{2Y}^2} - \overline{i_{1Y}^2} \\ \mathrm{Re}\,Z_{21} & \lvert Z_{21}\rvert^2\,\overline{i_G^2} + \lvert G_{22}\rvert^2\,\overline{i_{2Y}^2} - \lvert Z_{22}\rvert^2\,\overline{i_H^2} \end{vmatrix}$

4.3 Principle of Measurement of the Noisy Components of Linear Active Two-port

The set of noisy components of linear active two-port represented in each parameter are obtained uniquely by the calculation formulae in Section 4.2 if $\overline{i_{1Y}^2}$, $\overline{i_{2Y}^2}$, $\overline{i_H^2}$ and $\overline{i_G^2}$, or $\overline{v_{1Z}^2}$, $\overline{v_{2Z}^2}$, $\overline{v_H^2}$ and $\overline{v_G^2}$ are measured. The measurement of such noise sources are performed by current noise source method or voltage noise source method. The principle of measurements of $\overline{i_{1Y}^2}$, $\overline{i_{2Y}^2}$, $\overline{i_H^2}$ and $\overline{i_G^2}$ at the unit frequency band by comparing with standard noise current source is described in this section. The measurements of these noise current sources are performed in the same way except the difference of terminating conditions.

The internal noise of measuring equipment is expressed by the equivalent noise current source i_A as in Fig. 4.2, in which Z_A is the input impedance of the amplifier including the plate load of noise diode. The reading M_A of DCμA meter due to the detected current of output noise by the square law detector is given by

$$M_A = p\,\overline{i_A^2}\,Re\,Z_A \qquad (4.11)$$

where p is a proper constant determined by the amplifier system. $\overline{i_A^2}$ in Eq. 4.11 can be obtained as the noise current source supplied from the standard noise current source (noise diode) which indicates the double reading $2M_A$ of original reading. When the object to be measured is connected to the measuring equipment by switch S on, the reading of output meter becomes

$$M_T = p\left(\overline{i_A^2} + \overline{i_T^2}\right) Re\, \frac{Z_A Z_T}{Z_A + Z_T} \qquad (4.12)$$

Then the standard noise current source is supplied in order to increase the reading until the difference of $|M_T - M_A|$ is compensated. The reading is, then

$$M_D = p\left(\overline{i_A^2} + \overline{i_T^2} + \overline{i_D^2}\right) Re\, \frac{Z_A Z_T}{Z_A + Z_T} \qquad (4.13)$$

From Eqs. 4.11 through 4.13, we can obtain the noise current source $\overline{i_T^2}$ of the two-port. Namely, $\overline{i_T^2}$ is obtained by

$$\overline{i_T^2} = \overline{i_A^2}\left(\frac{|Z_A + Z_T|^2\, Re\, Z_A}{|Z_A|^2 Re\, Z_T + |Z_T|^2 Re\, Z_A} - 1\right) \pm \overline{i_D^2} \quad , \qquad (4.14)$$

where plus sign correspondes to $M_T > M_A$ and minus sign to $M_T < M_A$.

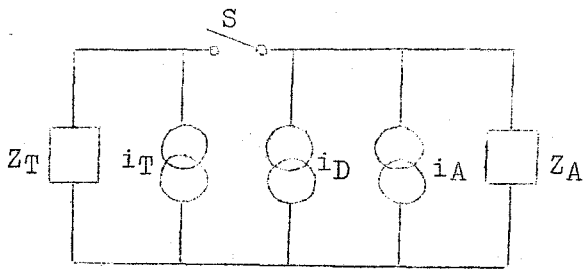

Fig. 4.2 High frequency noise equivalent circuit at the input terminal of measuring equipment.

4.4 Experimental Equipment to Measure the Noisy Components of a Linear Active Two-port

The experimental equipment which has been designed by author in order to measure the two-port noise of transistor at VHF band according to the principle described in Section 4.3 is presented here, with the measuring procedure and some notes on the actual measurement.

The blackdiagram of equipment is shown in Fig. 4.3. The quantities to be measured are the noise current sources $\overline{i_A^2}$ and $\overline{i_D^2}$, and the impedances Z_A and Z_T, from which $\overline{i_T^2}$ is calculated by Eq. 4.14.

Much attentions must be paid in arranging the mount of transistor and the low noise preamplifier attaching the standard noise diode in order to follow the principle described in previous section at VHF band. And they must be assembled in the manner that Z_A and Z_T are easily measured. The detail circuit diagram of this part is shown is Fig. 4.4. The open and short circuit conditions of transistor terminals are performed with the adjustable air line of Transfer and Immittance Function Meter (TIF meter) of General Ridio and the bias voltages are applied to trnsistor in its mount through the air line with low pass filter of TIF meter. The impedances Z_A and Z_T are measured by TIF meter. At impedance measurement, the effect of lead line near the switch circuit must be compensated and the high frequency by-pass condencer must be selected carefully. In order to measure accurately, the preamplifier must be adjusted so that $\overline{i_A^2}$ must be small value comparing with the noise source $\overline{i_T^2}$. The cascode connection constructed with available low noise vacuum tube is applied to the preamplifier. The noise figure of field intensity meter (main amplifier) is 13db at 70Mc and the total noise figure

improved by well adjusted preamplifer is 8db. The output noise at the intermediate frequency stage of field intensity meter is monitored by the 20μA meter through the square law detector. As the power gain of preamplifier is about 13db and the gain of field intensity meter and amplifier attached to detector are fairly high, the detected current can be measured satisfactorily by a 20μA meter.

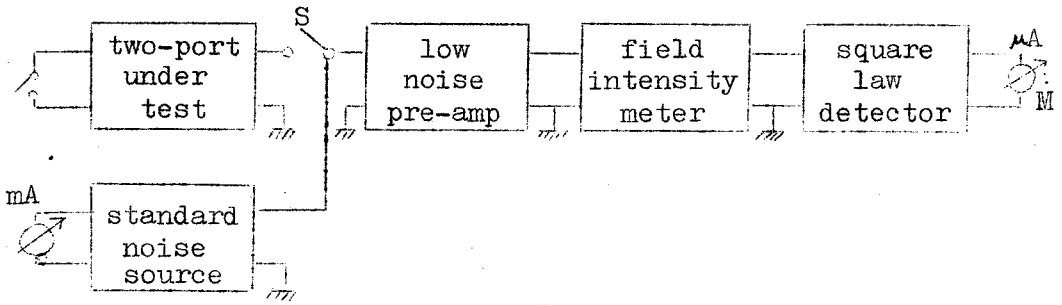

Fig. 4.3 Block diagram of experimental equipment to measure the internal noise sources of linear active two-port.

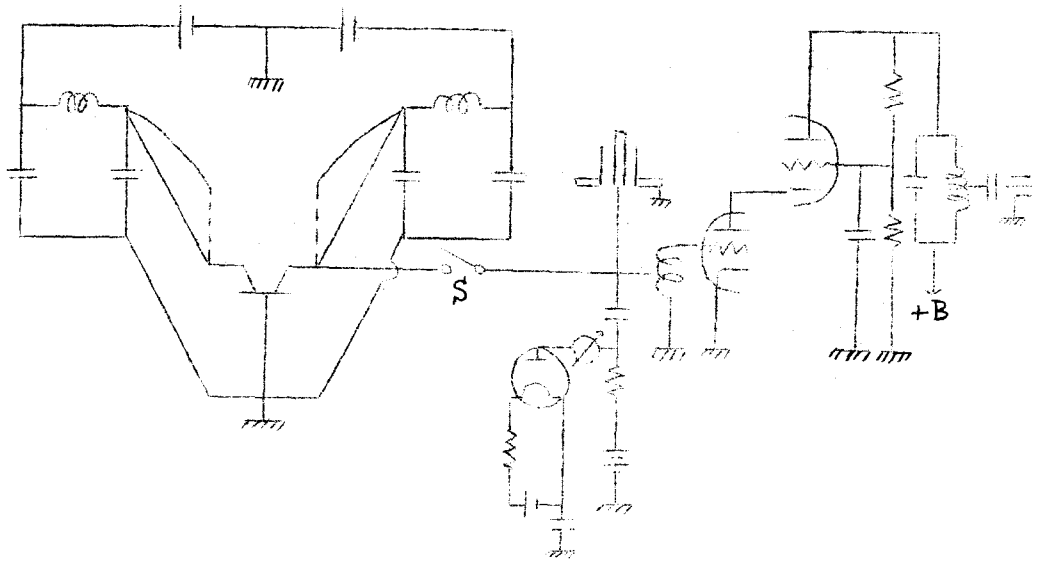

Fig. 4.4 Circuit diagram of low noise preamplifier.

The procedures of measurement are as follows;

1) Turn off the switch S and read the plate current I_L of standard noise diode by warming its heater so that the original reading of detected current is doubled, then we have

$$\overline{i_A^2} = 2e I_A \Delta f . \qquad (4.15)$$

2) Be sure to satisfy the terminating condition. Read both the output reading M_A when S is off and M_T when S is on. Add the standard noise

diode current I_D to be compensated the difference $|M_T - M_A|$, then we have

$$\overline{i_D^2} = 2e I_D \Delta f . \tag{4.16}$$

3) Measure the input impedance Z_A of the pre-amplifier and Z_T of two-port by TIF meter under the specified terminating condition.

4) Calculate the equivalent noise current source of the two-port from Eq. 4.14 using the measured results in the above procedures.

4.5 Two-port Noise of Transistor

The equivalent circuit of high frequency transistor including the internal noise sources is given by van der Ziel[24]-[26] and each noise source is specified.

The two-port noise of transistor can be obtained theoretically from the equivalent circuit of van der Ziel as follow;

$$\overline{v_F^2} = \overline{v_H^2} + \left|\frac{H_{11}}{H_{21}}\right|^2 \overline{i_H^2} - 2\,\mathrm{Re}\,\frac{H_{11}}{H_{21}}\,\overline{i_H v_H^*} \tag{4.17}$$

$$\overline{i_F^2} = \frac{\overline{i_H^2}}{|H_{21}|^2} \tag{4.18}$$

$$\overline{V_F i_F^*} = -\frac{\overline{V_H i_n^*}}{H_{21}^*} + \frac{\overline{i_H^2} H_{11}}{|H_{21}|^2} \tag{4.19}$$

where

$$V_H = e_e + \frac{e_b + i_c Z_b}{Z_c + Z_b} Z_c \tag{4.20}$$

$$i_H = \frac{i_c Z_c - e_b}{Z_b + Z_c} \tag{4.21}$$

$$\overline{e_e^2} = 2e I_E |Z_e|^2 \Delta f \tag{4.22}$$

$$\overline{e_b^2} = 4kT \Delta f \, Re\, Z_b \tag{4.23}$$

$$\overline{i_c^2} = 2e \left\{ (\alpha_0 - |\alpha|^2) I_E + I_{CO} \right\} \Delta f \tag{4.24}$$

$$\overline{e_e^* i_c} = 2kT \Delta f \, \alpha \left(G_{eo} - Y_e^* \right) \frac{1}{Y_e^*} \tag{4.25}$$

Z_b, $Z_e (= 1/Y_e)$, Z_c; base, emitter and collector impedance

G_{eo} ; emitter conductance at low frequency

The measured two-port current noise sources of junction transistor are shown in Fig. 4.5. These values are nearly equal to the theoretical values given from the equivalent circuit of van der Ziel. The

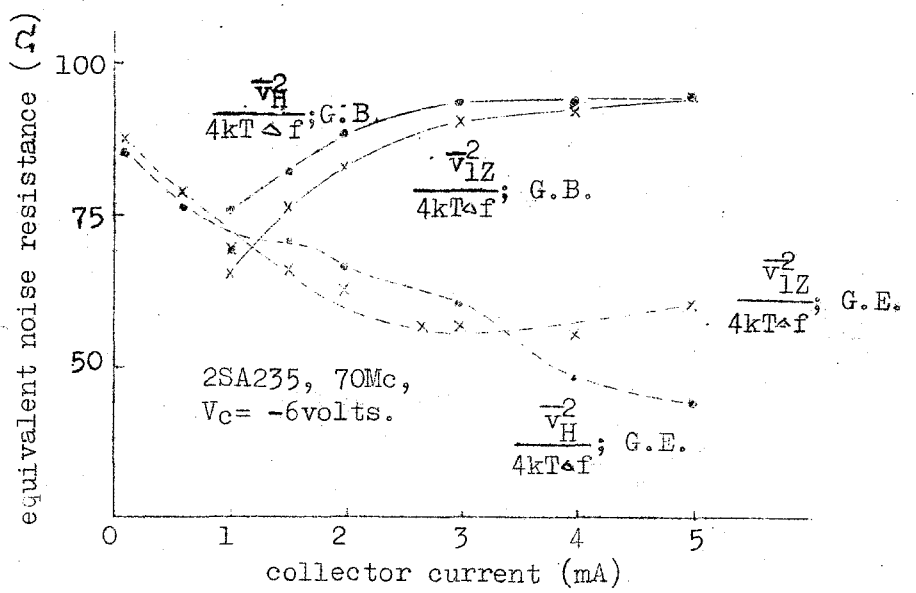

(a) noise source at input terminal

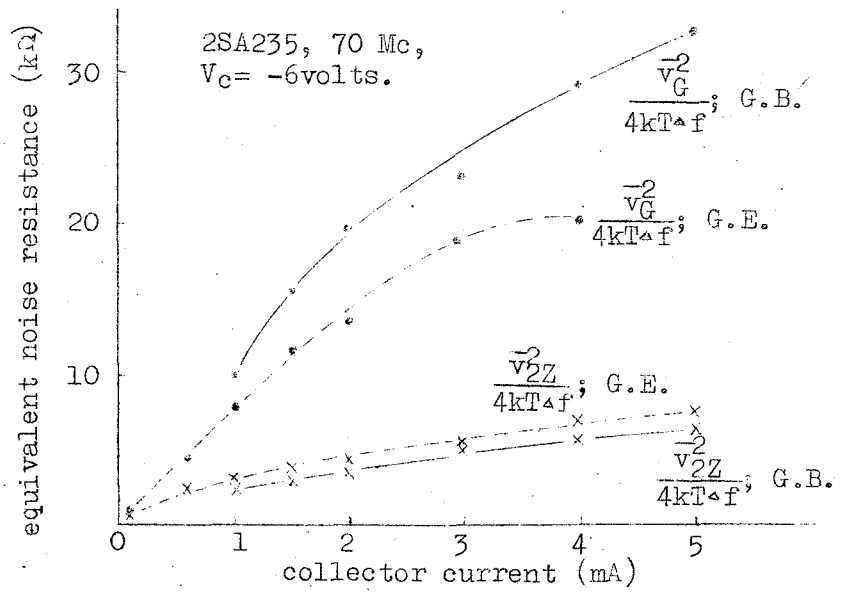

(b) noise source at output terminal

Fig. 4.5 Two-port noise sources of transistor, as dependent on collector current.

difference between them is caused by the difference between the actual transistor and the ideal transistor. When we want to use the set of noisy components of two-port, we had better use the measured values of actual two-port as we do when we use the circuit parameters. The sets of noisy components of junction transistor represented in F parameter are obtained by the transformation formulae from the measured noise current sources, which are shown in Fig. 4.6 and 4.7, in which the dependence of the noise current sources on the collector current and voltage is illustrated.

4.6 Summary of Chapter IV

The set of noisy components of linear active two-port can be measured directly by the comparison method with the standard noise source. The transformation formulae to obtain the set of noisy components from the short circuit noise current is introduced, from which we can calculate the set of noisy components after the measurement of the short circuit noise current sources.

The two-port noises of junction transistor have

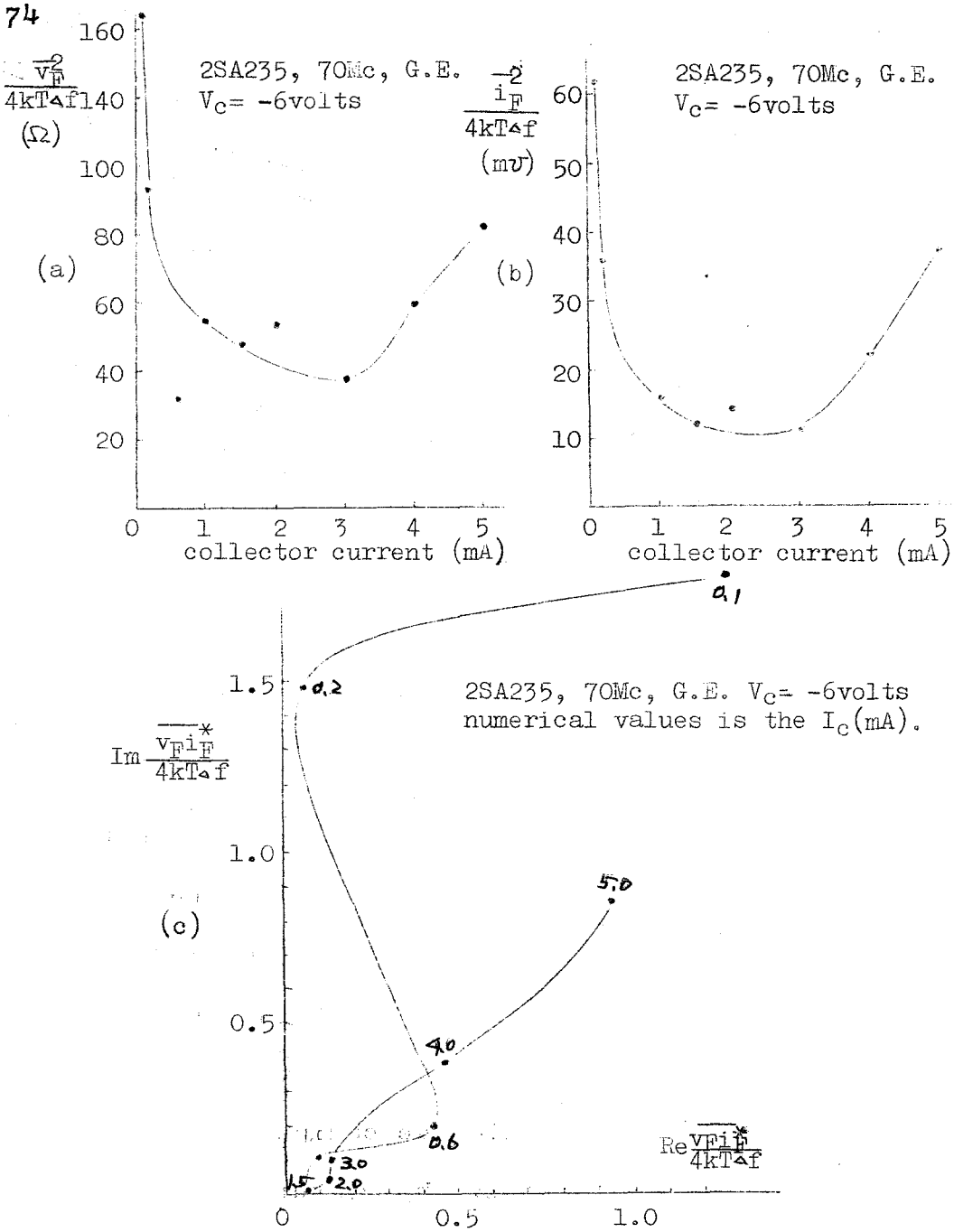

Fig. 4.6 The set of noisy components of junction transistor represented in F parameter, as dependent on collector current.

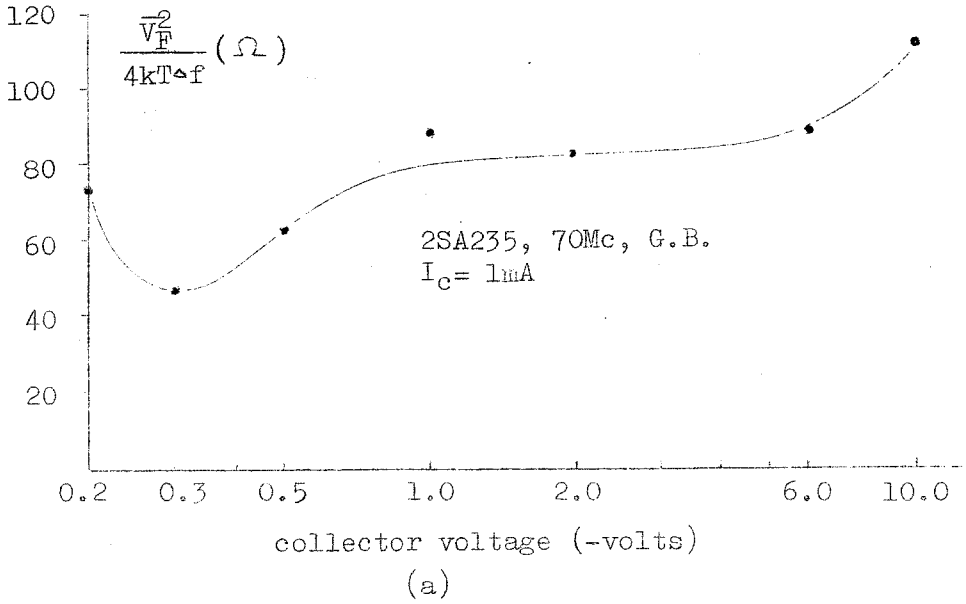
120
100
80
60
40
20
$\frac{\overline{V_F^2}}{4kT\Delta f}$ (Ω)
2SA235, 70Mc, G.B.
I_C= 1mA
0.2
0.3
0.5
1.0
2.0
6.0
10.0
collector voltage (-volts)

(a)

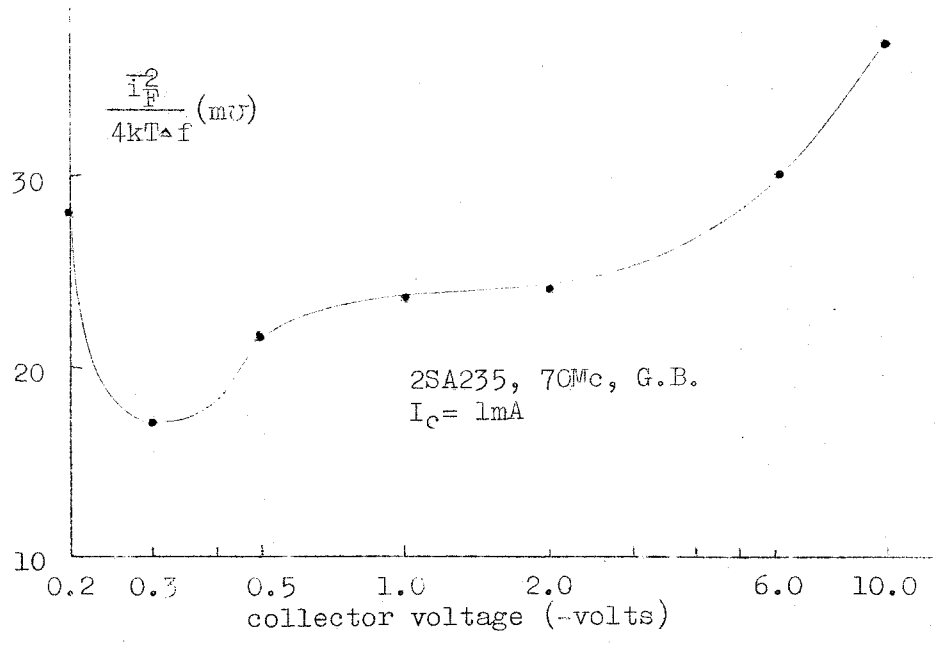
30
20
10
$\frac{\overline{i_F^2}}{4kT\Delta f}$ (mΩ)
2SA235, 70Mc, G.B.
I_C= 1mA
0.2
0.3
0.5
1.0
2.0
6.0
10.0
collector voltage (-volts)

(b)

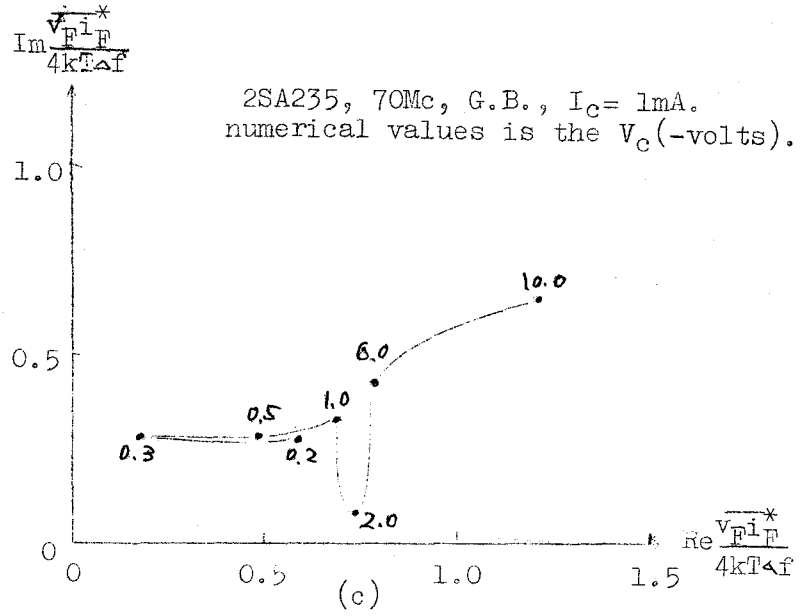

Fig. 4.7 The set of noisy components of junction transistor represented in F parameter, as dependent on collect voltage.

been measured by this method and the results of this measurements can be used for the estimation and the design of low noise amplifier as shown in Section 5.11.

CHAPTER V EXCHANGEABLE POWER GAIN AND EXCHANGEABLE NOISE MEASURE[34],[47],[48]

5.1 Preface

It is desirable to have high gain and low noise in an active two-port subject to a small signal. For each linear active two-port, there are the values of invariant power gain and noise measure for lossless transformation which determine the character of performance of the two-port. It is an important problem to know those invariant values and to realize them on the designing of an amplifier. In this chapter, the author carrys out the theoretical considerations on the exchangeable power gain G_e and the exchangeable noise measure M_e which has been defined by Haus and Adler[9]-[14] in

$$M_e = \frac{F_e - 1}{1 - 1/G_e} \tag{5.1}$$

as the criterion to estimate the noise performance of linear active two-port instead of the exchangeable noise figure F_e, with regard to,

1) the determinations of optimum values of the exchangeable power gain and noise measure, and their

realizations,

2) the determination and realization of the exchangeable power gain (or noise measure) when the exchangeable noise measure (or power gain) is optimum,

3) the realization of specified operating point below the optimum values,

4) the approximation method when the exchangeable power gain is large.

The noise measure has the common term with the iterative noise figure of Namekawa,[49] and it differs considerably from the conventional noise figure at the low gain stage of an amplifier. M_0 approaches F_e-1 when G_e becomes large.

The stationary problem of the exchangeable noise measure has been solved by Haus and Adler. However, it is necessary to attract attention to power gain as well as noise when we treat the active two-port. The author have obtained the stationary values of the exchangeable power gain from the eigenvalue of the characteristic gain matrix, and have applied the same argument to the exchangeable excess noise figure

which is useful at high gain stage of amplifier. The families of circles for constant exchangeable power gain, noise measure and noise figure are introduced, by which we can know the distributions of G_e, M_e and F_e graphically on the source impedance plane. Therefore, this chapter deals with the analysis and design theory with regard to the unsolved problems of the exchangeable power gain and noise measure.

Though there is a consideration for the contribution from the noise originating in, and reflected back to, the load,[16] only the effect of mismatching at the input side of an amplifier is considered here from the standpoint of Haus and Adler.

5.2 Eigenvalue Problem of Exchangeable Power Gain[47],[48]

The eigenvalue problem of the exchangeable power gain is described here, and it is shown that this method is similar to that of the exchangeable noise measure.

The exchangeable power gain is the ratio of the exchangeable power at the output of two-port to

that of source and is expressed by the ratio of Hermitian form. The stationary values of the ratio of Hermitian form are, if they are existent, obtained as the eigenvalues of proper operator by use of the Lagrange's multiplier method.[14] We shall hereafter name the operator for G_e as the characteristic gain matrix Γ and define it by

$$\Gamma = (F P F^{+})^{-1} P \,, \tag{5.2}$$

where

$$P = \begin{pmatrix} 0 & 1 \\ 1 & 0 \end{pmatrix} \tag{5.3}$$

and + means the Hermitian conjugate.

If $\det(F P F^{+})$ is not equal to zero, Γ is 2x2 matrix for a two-port. The case of $\det(F P F^{+})=0$ will be considered in Section 5.4. Let α denotes the eigenvalue of Γ, then we have

$$\Gamma y = \alpha y \,, \tag{5.4}$$

where

$$y = s\begin{pmatrix} 1 \\ Z_S^{*} \end{pmatrix}. \qquad s: \text{constant} \tag{5.5}$$

y is the eigenvector corresponding to the eigenvalue α. From Eq. 5.4, eigenvalues are obtained as

$$\alpha = \frac{\Gamma_{11} + \Gamma_{22} \pm \sqrt{(\Gamma_{11} + \Gamma_{22})^2 - 4(\Gamma_{11}\Gamma_{22} - \Gamma_{12}\Gamma_{21})}}{2}, \tag{5.6}$$

where Γ_{ij} $(i,j = 1,2)$ are the (i,j) components of Γ. The source impedances to realize α are obtained from

$$Z_S^{*})_\alpha = \frac{y_2}{y_1}\Big)_\alpha = \frac{\alpha - \Gamma_{11}}{\Gamma_{12}} = \frac{\Gamma_{21}}{\alpha - \Gamma_{22}} \tag{5.7}$$

as the ratio of the components of the eigenvector corresponding to α .

If the linear active two-port is not potentially unstable, the above mentioned eigenvalue of characteristic gain matrix is the well known complex conjugate matching power gain, and the source impedance to realize the complex conjugate matching power gain is obtained from the ratio of the components of eigenvector corresponding to the eigenvalue. These two arguments will be proved in Section 5.5. If the two-port is potentially unstable, the eigenvalue of characteristic gain matrix is not the real number, and the exchangeable power gain has not the stationary value. Therefore, in this case we can not realize the complex conjugate matching. The two-port of potential unstability means the two-port which the stable amplifier can be designed by using the suitable terminations. The problem concerning to the selection of terminations has been discussed in Chapter III.

On the other hand, the exchangable noise measure is also the ratio of Hermitian form. Haus and Adler named the operator for M_e as the charac-

teristic noise matrix,and shown that the eigenvalue of the characteristic noise matrix is the stationary value of M_e and the source impedance to realize M_e is the ratio of the components of the eigenvector. Therefore, the analytical method for M_e of Haus and Adler has been applied for Ge by author and it will also be applied for the exchangeable excess noise figure as shown in Section 5.10. They are able to be solved by the similar method.

5.3 Relation between Exchangeable Power Gain and Exchangeable Noise Measure[50]

The relation between exchangeable power gain and the exchangeable noise measure is considered here. For notational simplicity in the following, let

$$\left.\begin{aligned} a &= \mathrm{Re}\, F_{11} F_{12}^* \\ b &= \mathrm{Re}\, F_{21} F_{22}^* \\ c &= 1 - d/2 \\ d &= 2(F_{11} F_{22}^* + F_{12} F_{21}^*) \end{aligned}\right\} \qquad (5.8)$$

$$\left.\begin{aligned} \overline{v_F^2} &= 4kT\Delta f\, \Phi \\ \overline{i_F^2} &= 4kT\Delta f\, \Psi \\ \overline{i_F^* v_F} &= 4kT\Delta f\,(\Pi + j\Lambda) \end{aligned}\right\} \qquad (5.9)$$

where k is the Boltzmann constant, T is the absolute temperature and Δf is the equivalent bandwidth. The inverse of real part of d in Eq. 5.8 is the

complex conjugate matching power gain when the linear active two-port is reduced to unilateral by lossless reciprocal transformation. In this case, c and d are the invariants of this two-port for the lossless imbedding.

When the circuit parameter and the components of noise vector are used, G_e and M_e become

$$G_e = \frac{R_e Z_s}{b|Z_s|^2 + \frac{1}{2} R_e d^* Z_s + a} \tag{5.10}$$

$$M_e = \frac{\Phi |Z_s|^2 + 2R_e(\Pi - j\Lambda) Z_s + \Phi}{-b|Z_s|^2 + R_e c^* Z_s - a} \tag{5.11}$$

These equations are combined with the source impedance and give the gain and noise measure for an arbitrary source impedance.

After writing down in detail the components of the characteristic gain and noise matrices, we obtain

$$\alpha = \frac{R_e d \pm \sqrt{(R_e d)^2 - 4|\det \mathbb{F}|^2}}{2|\det \mathbb{F}|^2} \tag{5.12}$$

$$\Lambda = 2 \cdot \frac{a\Psi + b\Phi + R_e c(\Pi - j\Lambda) \pm \sqrt{[a\Phi + b\Psi + R_e c(\Pi - j\Lambda)]^2 + (|c|^2 - 4ab)(\Phi\Psi - \Pi^2 - \Lambda^2)}}{|c|^2 - 4ab} \tag{5.13}$$

Similary we have

$$Z_s^*)_\alpha = \frac{j I_m d \mp \sqrt{(R_e d)^2 - 4|\det \mathbb{F}|^2}}{4b} \tag{5.14}$$

$$Z_s^*)_\lambda = \frac{a\bar{T} - b\bar{\Pi} - jI_{mc}(\Pi - j\Lambda) \pm \sqrt{(a\bar{T} + b\bar{\Pi} + Re_c(\Pi - j\Lambda))_3^2 + (4c^2 - 4ab)(\bar{\Pi}\bar{T} - \Pi^2 - \Lambda^2)}}{2b(\Pi + j\Lambda) + c\bar{T}} \quad (5.15)$$

The stationary values α, λ of G_e, M_e are the invariants of a given two-port and used as a standard for the comparison of active two-port. The realizations of α and λ are possible by connections of the sources with the internal impedances determined by $Z_s^*)_\alpha$ and $Z_s^*)_\lambda$. As $Z_s^*)_\alpha$ are usually complex values different from $Z_s^*)_\lambda$, the amplifier which realize α and λ simultaneously by use of the given two-port may not be designed. At the design of amplifier, we may choose either α or λ , depending on we pay our relative attention to the gain or noise characteristics, respectively.

In order to design an optimum amplifier using the given linear active two-port, it is better to keep the noise measure at the optimum (lowest positive value) and connect it one by one, because the power gain can be considerably increased with multistage; namely make the source impedance and the output impedance of the first stage to be $Z_s^*)_\lambda$ and connect it to the second stage. The values of G_e when M_e is stationary can be calculated by substituting Eq.5.13

into Eq.5.10. If this value of G_e is larger than unity, the exchangeable power gain can be made fairly large by the above mentioned multistage. In this case, it is known that M_e does not descrease from the optimum value of unit stage. In addition, the values of M_e when G_e is stationary can be calculated by putting Eq. 5.14 into Eq. 5.11.

The active two-port with a large positive α and a small positive λ is desirable for the design of an amplifier with regard to G_e and M_e , when Z_S corresponding to those values are adjacent and easily realized.

5.4 Singular Cases of Characteristic Matrices

The characteristic gain matrix is singular for unilateral two-port. A given nonreciprocal two-port can be reduced to the two-port with singular $\mathbb{F}$, because ~~any~~ the two-port can be reduced to the unilateral by lossless reciprocal transformation. For the unilateral two-port or the reduced unilateral two-port by lossless reciprocal imbedding, the stationary value of the exchangeable power gain α_0 and the source impedance to realize it are given by solving

$$\mathbf{P}_y = \alpha_0 (\mathbf{F}\mathbf{P}\mathbf{F}^+)_y \qquad (5.16)$$

under the condition of $\det \mathbf{F} = 0$ as

$$\alpha_0 = \frac{1}{Re\, d} \qquad (5.17)$$

$$Z_s^*)_{\alpha_0} = \frac{F_{11}}{F_{21}} = \frac{F_{12}}{F_{22}} . \qquad (5.18)$$

α_0 coincides with the unilateral gain given by Eq. 2.6 at $\det \mathbf{F} = 0$.

The characteristic noise matrix of a two-port with the F parameter as

$$\begin{pmatrix} 1 & Z \\ 0 & 1 \end{pmatrix}, \quad \begin{pmatrix} 1 & 0 \\ Y & 1 \end{pmatrix}, \quad \begin{pmatrix} W & 1 \\ 1 & 0 \end{pmatrix}, \quad \begin{pmatrix} 0 & 1 \\ 1 & V \end{pmatrix} \qquad (5.19)$$

is singular. In these cases, the stationary value of noise measure λ_0 and the source impedance to realize it are given by solving

$$\frac{\overline{\delta\delta}}{2kT_0 f}\, y = \lambda_0 (\mathbf{P} - \mathbf{F}\mathbf{P}\mathbf{F}^+) y , \qquad (5.20)$$

where $\delta = \begin{pmatrix} v_F \\ i_F \end{pmatrix}$

under the condition of $\det (\mathbf{P} - \mathbf{F}\mathbf{P}\mathbf{F}^+) = 0$ as

$$\lambda_0 = \frac{\Pi^2 + \Lambda^2 - \Phi\Psi}{a\Psi + b\Phi + Re\, c(\Pi - j\Lambda)} \qquad (5.21)$$

$$Z_s^*)_{\lambda_0} = - \frac{a(\Pi^2 + \Lambda^2) + b\Phi^2 + \Phi\, Re\, c(\Pi - j\Lambda)}{(a\Psi + b\Phi)(\Pi + j\Lambda) + \frac{c\Phi\Psi + c^*(\Pi + j\Lambda)^2}{2}} . \qquad (5.22)$$

When the denominator of Eq. 5.21 is zero, there is no stationary value. The amplifiers with negative resistance are included in this case and the exchangeable noise measure of negative resistance

amplifiers is known to be a constant, $\frac{-P_e}{kT\Delta f}$, (15) where P_e is the exchangeable power of negative resistance.

5.5 Complex Conjugate Matching (51)

Though the concept of complex conjugate matching power gain is well known, we will discuss the complex conjugate matching at the input and the output of an amplifier in order to understand the physical meaning of the stationary gain which has been obtained in Section 5.2. The power gain G_{match} and the input impedance Z_{in} under the conditions of

$$Z_S = Z_{in}^* \tag{5.23}$$

$$Z_L = Z_{out}^* \tag{5.24}$$

are given by

$$G_{match} = \frac{|Z_{21}|^2}{|Z_{22} + P - jQ|^2} \cdot \frac{Re\,Z_{22}}{Re\,Z_{11}} \tag{5.25}$$

$$Z_{in} = \frac{j(2Re\,Z_{22}\,Im\,Z_{11} - Im\,Z_{12}Z_{21}) \mp \sqrt{(2Re\,Z_{11}Re\,Z_{22} - Re\,Z_{12}Z_{21})^2 - |Z_{12}Z_{21}|^2}}{2\,Re\,Z_{22}} \tag{5.26}$$

where

$$P = \frac{\sqrt{(2Re\,Z_{11}Re\,Z_{22} - Re\,Z_{12}Z_{21})^2 - |Z_{12}Z_{21}|^2}}{2\,Re\,Z_{11}} \tag{5.27}$$

$$Q = \frac{2\,Re\,Z_{11}\,Im\,Z_{22} - Im\,Z_{12}Z_{21}}{2\,Re\,Z_{11}} \,. \tag{5.28}$$

The α in Eq. 5.12 is related to Gmatch in Eq. 5.25 by

$$G_{match} = \alpha \,, \tag{5.29}$$

and there is a relation between Z_{in} of Eq. 5.26 and $Z_S^*)_\alpha$ of Eq. 5.14 as

$$Z_{in} = Z_S^*)_\alpha \,. \tag{5.30}$$

Therefore, it is clarified that the stationary values of the exchangeable power gain given by the eigen-values of characteristic gain matrix in Section 5.2 are the complex conjugate matching power gain and that $Z_S)_\alpha$ are the source impedances which realize them. This is also true for an unilateral two-port. Here, the loads in the case of complex conjugate matching at the input and the output side of an amplifier are given in

$$Z_L = \frac{-j(2\,Re\,Z_{11}\,I_m\,Z_{11} - I_m\,Z_{12}\,Z_{21}) \mp \sqrt{(2\,Re\,Z_{11}\,Re\,Z_{22} - Re\,Z_{12}\,Z_{21})^2 - |Z_{12}\,Z_{21}|^2}}{2\,Re\,Z_{11}} \,. \tag{5.31}$$

The double signs in Eqs. 5.6, 5.12, 5.14, 5.25 and 5.31 are effective in same order.

Applying the similar consideration to the noise measure, we can refer the realization of the optimum Me as the complex conjugate matching of noise measure.(51)

5.6 Characteristics of Exchangeable Power G in

In order to know the characteristics of the exchangeable power gain when the source impedance is varied, we have

$$G_e = \frac{R_S}{b\left\{\left(R_S + \frac{Red}{4b}\right)^2 + \left(X_S + \frac{Imd}{4b}\right)^2 - \frac{|\det F|^2}{4b^2}\right\}} \qquad (5.32)$$

by putting $Z_S = R_S + jX_S$ into Eq. 5.10. The locus for the equation which is obtained making the denominator of Eq. 5.32 zero becomes a circle on the source impedance plane, if the equation is for bilateral two-port and namely the characteristic gain matrix is not singular, where

$$\text{radius;} \quad \frac{|\det F|}{2|b|} \qquad (5.33)$$

$$\text{center;} \begin{cases} R_S = -\dfrac{Red}{4b} & (5.34) \\ X_S = -\dfrac{Imd}{4b} \,. & (5.35) \end{cases}$$

The radius for unilateral two-port is zero and the circle is reduced to a point.

This circle does not intersects the X_S axis when $2|\det F| < |Red|$ which corresponds to $|K| < 1$ in Section 3.5, that is, when the linear active two-port is not

potentially unstable, and intersects the X_S axis when the two-port is potentially unstable which corresponds to $|K|>1$. When $|K|=1$, the circle is tangent to the X_S axis.

Table 3 shows the sign of G_e in Eq. 5.32. G_e represents a surface whose height is uniquely determined by Eq. 5.32 for each point in the source impedance plane. Thus a curve of G_e can be drawn after drawing the above mentioned circle and fixing R_S or X_S on arbitrary value.

Table 3 Signs of G_e and M_e .

G_e	R_S	+		−	
	b	+	−	+	−
	inside the circle	−	+	+	−
	on the circle	pole			
	outside the circle	+	−	−	+
M_e	$\det(P-FPF^+)$	−		+ , 0	
	b	+	−	+	−
	inside the circle	+	−	− , + (or pole)	
	on the circle	pole			
	outside the circle	−	+		

5.7 Family of Circles for Constant Exchangeable Power Gain[34],[38],[47],[48],[52]

In order to know the distribution of the exchangeable power gain on the source impedance plane, we have

$$\left\{R_s+\frac{1}{4b}\left(Red-\frac{2}{G_e}\right)\right\}^2+\left(X_s+\frac{Im\,d}{4b}\right)^2=\frac{G_e^2|\det F|^2-G_e Red+1}{4b^2G_e^2} \qquad (5.36)$$

for a fixed values of G_e. The locus of Eq. 5.36 shows the family of circles for constant G_e on the source impedance plane when the right hand side of Eq. 5.36 is positive, where

$$\text{radii;}\quad \frac{\sqrt{G_e^2|\det F|^2-G_e Red+1}}{2|bG_e|} \qquad (5.37)$$

$$\text{centers;}\quad \begin{cases} R_s=\dfrac{1}{2G_eb}-\dfrac{Red}{4b} & (5.38)\\[2ex] X_s=-\dfrac{Im\,d}{4b}. & (5.39)\end{cases}$$

Eqs. 5.37, 5.38 and 5.39 are reduced to Eqs. 5.33 5.34 and 5.35 respectively when G_e approaches infinity. The center moves in parallel with R_s axis as G_e varies.

The ranges of G_e are specified by the condition that the right hand side of Eq. 5.36 be non-

negative as in Table 4. In this table, $\det F \neq 0$ is the case of bilateral two-port and $\det F = 0$ is that of unilateral two-port. $|\mathrm{Re}\,d| > 2|\det F|$ is the case of $1 > |K|$, that is not potentially unstable (if $\mathrm{Re}\,H_{22} > 0$), $|\mathrm{Re}\,d| \leq 2|\det F|$ is case of $1 \leq |K|$, that is the case of potentially unstable, as described in Section 3.5. When $\mathrm{Re}\,d > 0$ for the unilateral two-port, the real part of input and output immittances are both positive or negative, and when $\mathrm{Re}\,d < 0$, one of them is positive and the other is negative. The α_0, α_1 and α_2 ($\alpha_2 > \alpha_1$) of Table 4 are the solutions of equation which is obtained by making the right hand side of Eq. 5.36 zero, and α_0 coincides with the stationary value of Eq. 5.17 and α_1, α_2 coincide with the eigenvalues of Eq. 5.12. At the stationary values α_0, α_1 and α_2 of G_e, the radius of circle for constant G_e is reduced to zero. When the two-port is bilateral R_S corresponding to α_1 and α_2 are located symmetrically with respect to X_S axis, and when it is unilateral R_S to α_0 and the pole of G_e are also located symmetrically with respect to X_S axis, and the center of circle for constant G_e is not existent between them respec-

tivelly.

Through these considerations, the family of circles for constant exchangeable power gain on the complex source impedance plane and its cross section for a given linear active two-port can be drawn as illustrated in Fig. 5.1. At the design of an amplifier, it is convenient to select the input circuit according to the chart.

Tabel 4 Ranges of G_e and M_e.

G_e	$\det F \neq 0$	$\lvert \mathrm{Red} \rvert > 2\lvert \det F \rvert$	$G_e \geq \alpha_2, \alpha_1 \geq G_e$
		$\lvert \mathrm{Red} \rvert \leq 2\lvert \det F \rvert$	G_e may take all the values.
	$\det F = 0$	$\mathrm{Red} > 0$	$\alpha_0 \geq G_e$
		$\mathrm{Red} < 0$	$G_e \geq \alpha_0$
M_e	$\det(P - FPF^+) < 0$	$M_e \geq \lambda_2$, $\lambda_1 \geq M_e$	
	$\det(P - FPF^+) > 0$	$\{a\Psi + b\Phi + \mathrm{Re}\, c(\Pi - j\Lambda)\}^2 > (\lvert c \rvert^2 - 4ab)(\Pi^2 + \Lambda^2 - \Phi\Psi)$	$\lambda_2 \geq M_e \geq \lambda_1$
		$\{a\Psi + b\Phi + \mathrm{Re}\, c(\Pi - j\Lambda)\}^2 \leq (\lvert c \rvert^2 - 4ab)(\Pi^2 + \Lambda^2 - \Phi\Psi)$	There is no value of M_e.
	$\det(P - FPF^+) = 0$	$a\Psi + b\Phi + \mathrm{Re}\, c(\Pi - j\Lambda) > 0$	$\lambda_0 \geq M_e$
		$a\Psi + b\Phi + \mathrm{Re}\, c(\Pi - j\Lambda) < 0$	$M_e \geq \lambda_0$

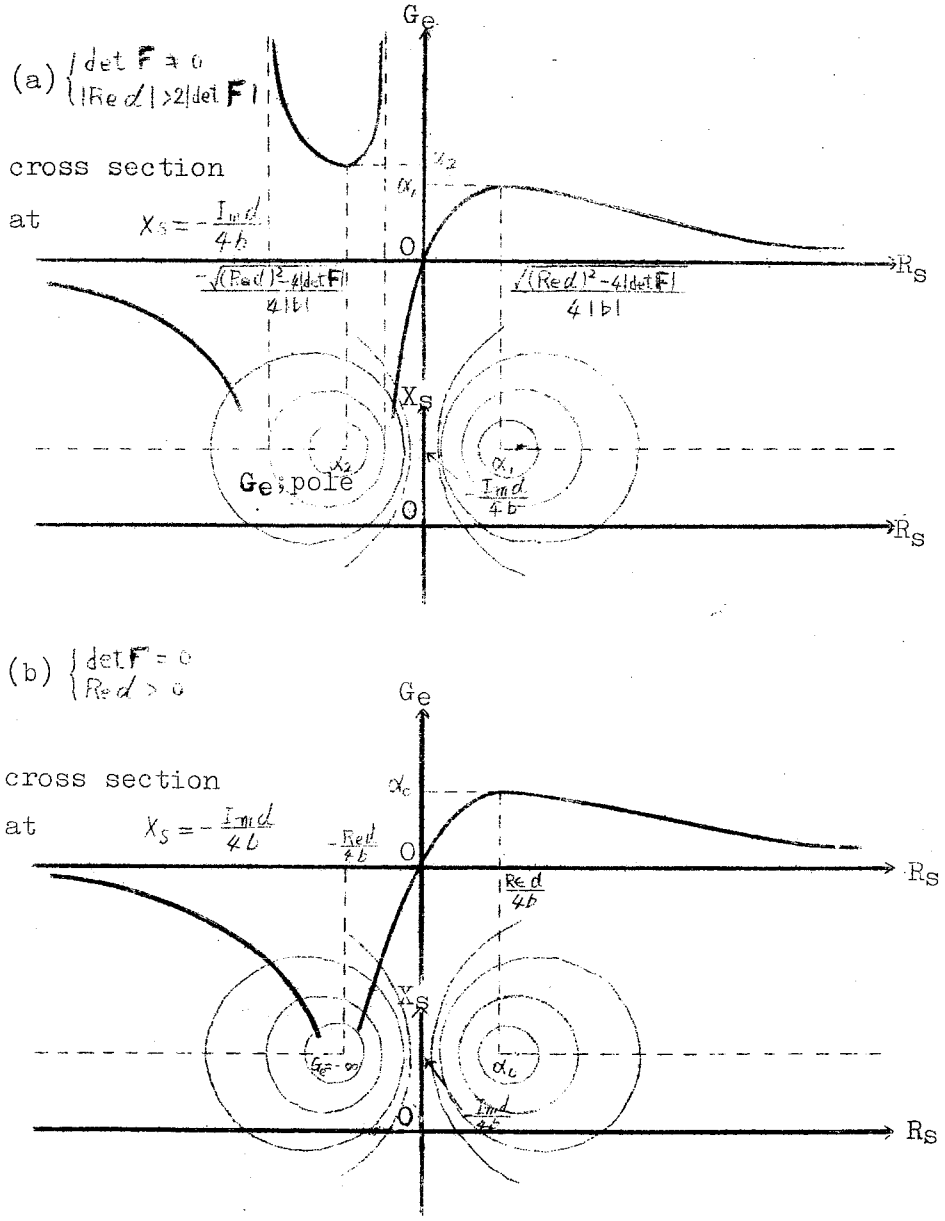

Fig. 5.1 Loci of constant exchangeable power gain and its cross section.

5.8 Characteristics of Exchangeable Noise Measure

In order to know the characteristics of the exchangeable noise measure when the source impedance is varied, we have

$$M_e = \frac{\Psi\left(R_S + \frac{\Pi}{\Psi}\right)^2 + \Psi\left(X_S + \frac{\Lambda}{\Psi}\right)^2 + \frac{\Phi\Psi - (\Pi^2 + \Lambda^2)}{\Psi}}{-b\left\{\left(R_S - \frac{Re\,c}{2b}\right)^2 + \left(X_S - \frac{Im\,c}{2b}\right)^2 - \frac{|c|^2 - 4ab}{4b^2}\right\}} \qquad (5.40)$$

by putting $Z_S = R_S + jX_S$ into Eq. 5.11. If the sign of

$$det(P - FPF^+) \equiv -|c|^2 + 4ab \qquad (5.41)$$

for a given two-port is positive, the sign of the inside of the bracket in Eq. 5.40 is always positive, and the noise measure is not infinite and the power gain is not larger than unity for the source impedance outside the circle of infinity G_e. When the sign of Eq. 5.41 is negative, the locus for the equation which is obtained making the denominator of Eq. 5.40 zero makes a circle on the source impedance plane, where

$$\text{radius;} \quad \frac{\sqrt{|c|^2 - 4ab}}{2|b|} \qquad (5.42)$$

$$\text{center;} \quad \begin{cases} R_S = \dfrac{Re\,c}{2b} & (5.43) \\ X_S = \dfrac{Im\,c}{2b} & (5.44) \end{cases}$$

If the two-port includes negative resistances or is composed of one element, that is $\det(P-FPF^{+})=0$, the radius of above circle is zero.

This circle does not intersect the X_S axis when $\sqrt{|c|^2-4ab} < |Re\,d|$ which corresponds to $|K|<1$ in Section 3.5, that is, when the linear active two-port is not potentially unstable, (if $Re\,H_{22}>0$) and intersects the X_S axis when the two-port is potentially unstable which corresponds to $|K|>1$. When $|K|=1$, the circle is tangent to the X_S axis.

From Eq. 5.40 we have

$$M_e \text{ at } R_S=X_S=0 = -\frac{\Phi}{a} \tag{5.45}$$

$$\lim_{R_S\to\pm\infty} M_e = \lim_{X_S\to\pm\infty} M_e = -\frac{\Psi}{b} \; . \tag{5.46}$$

On the other hand, if v_F has not a complete correlation with i_F , that is

$$\Phi\Psi > \Pi^2 + \Lambda^2 , \tag{5.47}$$

the numerator of Eq. 5.40 has a positive value.

Table 3 shows the sign of M_e in Eq. 5.40. M_e represents a surface whose height is uniquely determined by Eq. 5.40 for each point in the source impedance plane. Thus a curve of M_e can be drawn after drawing the above mentioned circle and fix-

ing R_S or X_S on arbitrary value.

5.9 Family of Circles for Constant Exchangeable Noise Measure (34),(38),(47),(48),(52)

In order to know the distribution of the exchangeable noise measure on the source impedance plane, we have

$$\left(R_S + \frac{B}{2A}\right)^2 + \left(X_S + \frac{C}{2A}\right)^2 = \frac{B^2 + C^2 - 4AD}{4A^2} \qquad (5.48)$$

for a fixed value of M_e , where

$$\left.\begin{aligned} A &= \Psi + M_e b \\ B &= 2\Pi - M_e R_{ec} \\ C &= 2\Lambda - M_e I_{mc} \\ D &= \Phi + M_e a \end{aligned}\right\} \qquad (5.49)$$

The locus of Eq. 5.48 shows the family of circles for constant M_e on the source impedance plane when the right hand side of Eq. 5.48 is positive, where

$$\text{radii;} \quad \frac{\sqrt{B^2 + C^2 - 4AD}}{2|A|} \qquad (5.50)$$

$$\text{centers;} \quad \left\{ \begin{aligned} R_S &= \frac{M_e R_{ec} - 2\Pi}{2(M_e b + \Psi)} && (5.51) \\ X_S &= \frac{M_e I_{mc} - 2\Lambda}{2(M_e b + \Psi)} . && (5.52) \end{aligned}\right.$$

Eqs. 5.50, 5.51 and 5.52 are reduced to Eqs. 5.42, 5.43 and 5.44 respectively when M_e approaches infinity. The locus of the centers as M_e varies is given from Eqs. 5.51 and 5.52 as

$$R_s(\Psi I_{mc}+2\Lambda b)-X_s(\Psi R_{ec}+2\Pi b)+\Pi I_{mc}-\Lambda R_{ec}=0. \quad (5.53)$$

The locus of infinity Me specified by Eq. 5.46 is a line on the source impedance plane given by

$$R_s(\Psi R_{ec}+2\Pi b)+X_s(\Psi I_{mc}+2\Lambda b)+b\Phi-a\Psi=0. \quad (5.54)$$

Equation 5.53 is orthogonal to Eq. 5.54 and the cross point is the center point of the two Z_s which are given in Eq. 5.15.

The ranges of Me are specified by the condition that the right hand side of Eq. 5.48 be non-negative as in Table 4. In this table, $\det(P-FPF^+)\neq 0$ is the nonsingular case of characteristic noise matrix and $\det(P-FPF^+)=0$ is the singular case of it. The negative resistance amplifiers are included in the later case if $a\Psi+b\Phi+R_{ec}(\Pi-j\Lambda)=0$.

The M_e of negative resistance amplifiers is a constant, $-\frac{P_e}{kT\Delta f}$ as obtained from Eq. 5.11, which does not depend on the particular source impedance. This results is agreed with the report of Penfield[15],

which is the special case of this theory. The λ_0, λ_1 and $\lambda_2(\lambda_2 > \lambda_1)$ of Table 4 are the solutions of equation which is obtained by making the right hand side of Eq. 5.48 zero, and λ_0 coincides with the stationary value of Eq. 5.21 and λ_1, λ_2 coincides with the eigenvalues of Eq. 5.13. At the stationary values of λ_0, λ_1 and λ_2 of M_e, the radius of the circles for constant M_e is reduced to zero. When the characteristic noise matrix is not singular Z_S corresponding to λ_1 and λ_2 are located symmetrically with respect to the line of Eq. 5.54 and when the two-port includes negative resistance or is composed of one element Z_S to λ_0 and the pole of M_e are also located symmetrically with respect to Eq. 5.54 and the center of circle for constant M_e is not existent between them respectively.

Through these considerations, the family of circles for constant exchangeable noise measure on the complex source impedance plane and its cross section for a given linear active two-port can be drawn as illustrated in Fig. 5.2. The circle of unity G_e in Fig. 5.1 coincides with the circle of infinity M_e in Fig. 5.2, and M_e is positive when

G_e is larger than unity for the range of positive R_S; this is also supposed from the definition of M_e. Therefore, at the design of an amplifier with positive R_S it must be used the source impedance inside the circle of unity G_e.

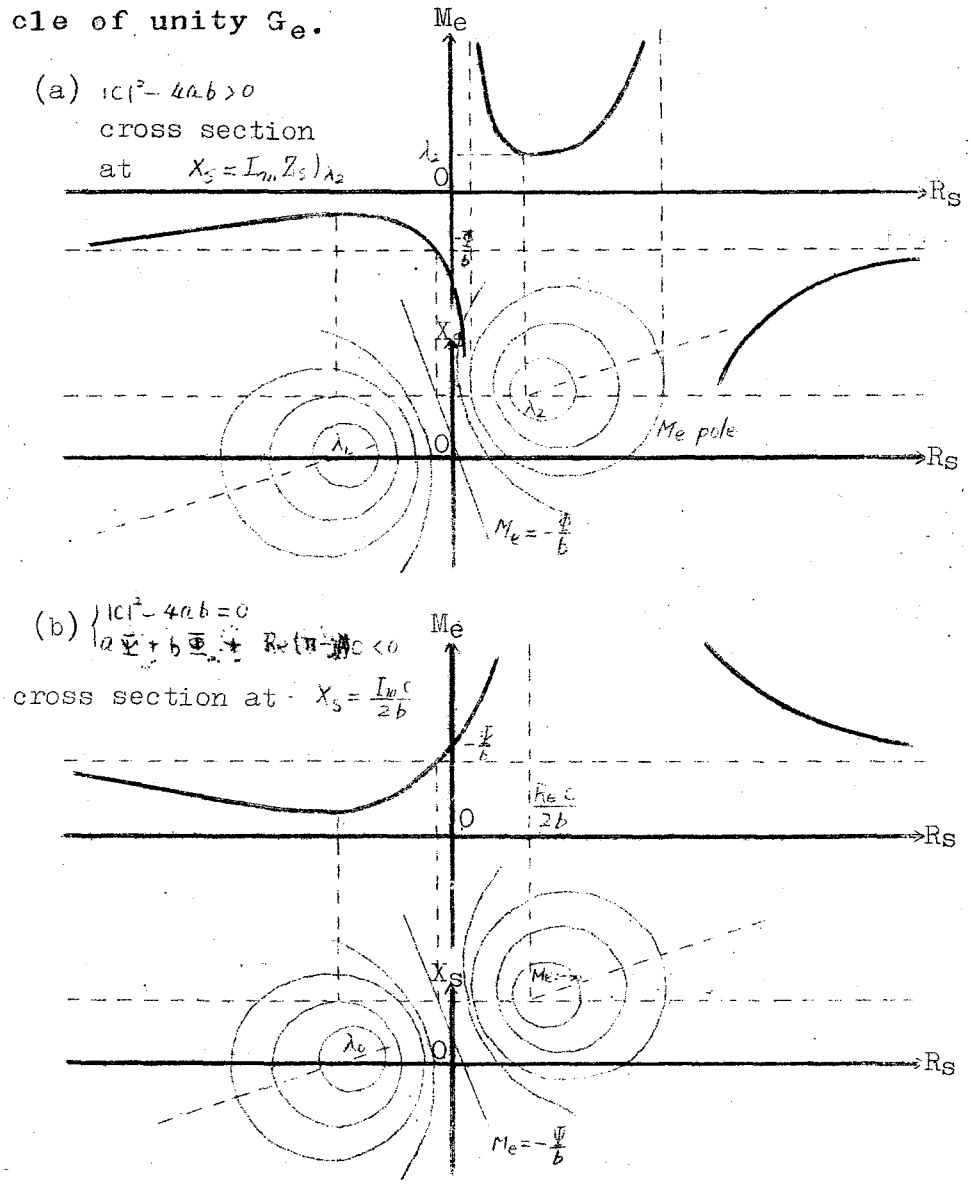

Fig. 5.2 Loci of constant exchangeable noise measure and its cross section.

5.10 Exchangeable Excess Noise Figure[47],[48]

The noise measure approaches the excess noise figure when the power gain becomes large. It is better to use the following excess noise figure instead of noise measure when the high gain, in actual, larger than about 10 db is obtained.

As the exchangeable excess noise figure F is also given by the ratio of Hermitian form, the similar treatments as G_e and M_e are applied to F. The author define the characteristic noise figure matrix N' as

$$N' = \frac{1}{2kT_0 f} \cdot P^{-1} \delta \delta^{+} \qquad (5.55)$$

The eigenvalues λ' of N' can be obtained from

$$N'y = \lambda' y \ , \qquad (5.56)$$

that is,

$$\lambda' = 2\Pi \pm 2\sqrt{\Phi\Psi - \Lambda^2} \ . \qquad (5.57)$$

The characteristic noise figure matrix N' is non-singular and $(\Phi\Psi - \Lambda^2)$ is always positive. The eigenvalues λ' are the stationary values of F and the source impedances to realize them are obtained as the ratios of components of the eigen-

vectors for these eigenvalues by

$$Z_s^*)_\chi = \frac{\pm\sqrt{\Xi\Psi - \Lambda^2} + j\Lambda}{\Psi} \quad . \qquad (5.58)$$

The realization of the optimum value of F is the complex conjugate matching of the exchangeable excess noise figure.

The exchangeable excess noise figure is expressed by

$$F = \frac{\Psi\left(R_s + \frac{\Pi}{\Psi}\right)^2 + \Psi\left(X_s + \frac{\Lambda}{\Psi}\right)^2 + \frac{\Xi\Psi - (\Pi^2+\Lambda^2)}{\Psi}}{R_s} \qquad (5.59)$$

as the function of source impedance and the components of noise vector. The sign of R_s is same to that of F because the numerator of Eq. 5.59 is non-negative. From Eq. 5.59 we obtain

$$\left(R_s + \frac{2\Pi - F}{2\Psi}\right)^2 + \left(X_s + \frac{\Lambda}{\Psi}\right)^2 = \frac{F^2 - 4\Pi F + 4(\Pi^2+\Lambda^2-\Xi\Psi)}{4\Psi^2} \qquad (5.60)$$

for a fixed value of F. The locus of Eq. 5.60 shows the family of circles for constant F on the source impedance plane when the right hand side of Eq. 5.60 is positive, that is,

$$F \geq \lambda_2' \quad , \qquad \lambda_1' \geq F \qquad (\lambda_2 > \lambda_1') \qquad (5.61)$$

where radii; $\frac{\sqrt{F^2 - 4\Pi F + 4(\Pi^2+\Lambda^2-\Xi\Psi)}}{2\Psi}$ (5.62)

centers;
$$\begin{cases} R_S = \dfrac{F - 2\pi}{2\Phi} & (5.63) \\ X_S = -\dfrac{\Lambda}{\Phi} . & (5.64) \end{cases}$$

The λ_1' , λ_2' in Uneq. 5.61 coincide with the eigenvalues of Eq. 5.57. At the stationary values of λ_1' and λ_2', the radius of the circles for sonstant F is reduced to zero. R_S corresponding to λ_1 and λ_2 are located symmetrically with respect to X_S axis.

Through these considerations, the family of circles for constant exchangeable excess noise figure and its cross section can be drawn as in Fig. 5.3. They will be also used in the design of amplifiers.

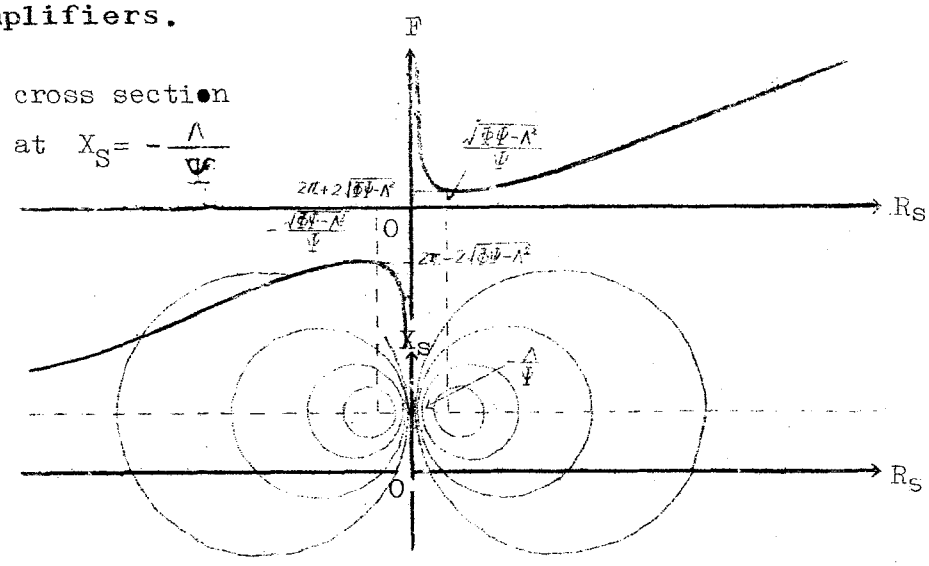

Fig. 5.3 Loci of constant exchangeable excess noise figure and its cross section.

5.11 Application to Transistor Amplifiers

In this section the previously mentioned general theory is applied to the high frequency transistor amplifiers. At the design of low noise amplifiers using the given transistor, we need to know the available limit of power gain and noise measure (or noise figure), and their realization methods.

The transistor 2SA235 is used here in grounded base configuration at 70Mc, V_c=-6 volts. The maximum power gains and the source impedances to realize them by the use of this transistor at 100 Mc are shown in Section 3.7. As the maximum power gain of the transistor at 100 Mc is sufficiently high (α_1=14db at V_c=-6 volts, I_c=2mA, G.B.), we had better, in this case, use the exchangeable noise figure as the criterion to estimate the noise performance of the amplifier. The curves of the optimum values of exchangeable excess noise figure and the source impedances to realize them, calculated from the measured circuit parameters and the set of noisy components given in Section 4.5 are shown in Figs. 5.4 and 5.5.

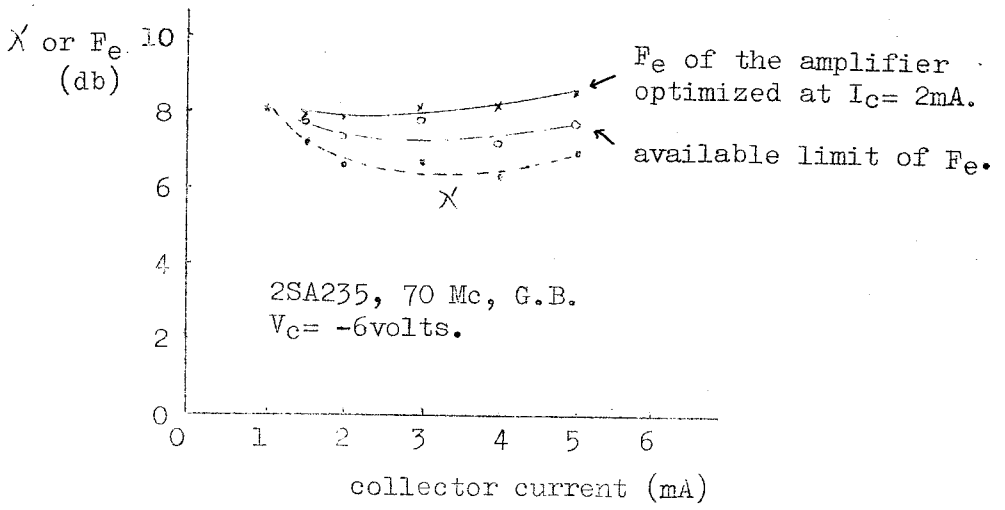

Fig. 5.4 Curves of λ' and available limit of F_e calculated from the circuit parameters and the set of noisy components, as dependent on collector current, together with the experimental results of F_e optimized at I_c=2mA.

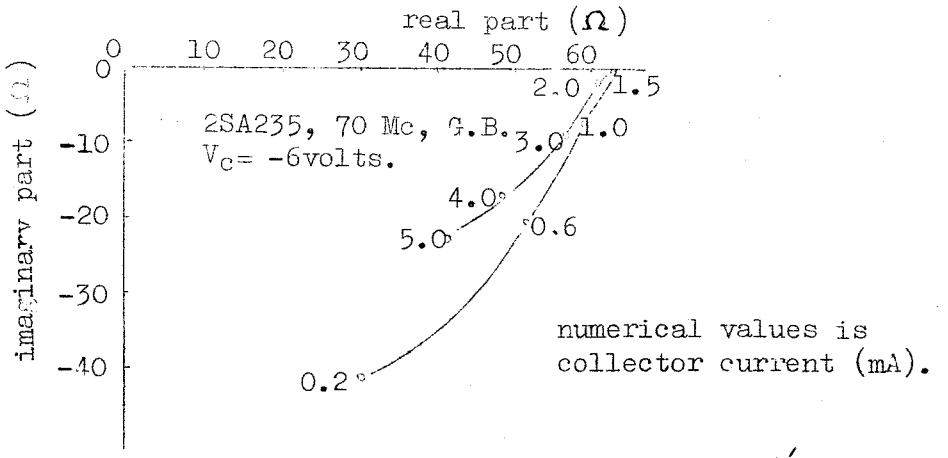

Fig. 5.5 Scurce Impedances to realize λ' as dependent on collector current.

The curve of exchangeable noise figure of the amplifier optimized at I_c=2mA is also shown in Fig. 5.4, together with the curve of available limit (optimum value) of noise figure calculated from the curve of λ'. As the experimental results of the exchangeable power gain is fairly high (18.6db) when the noise figure is optimized, the exchangeable noise figure shown in Fig. 5.6 is significant on the evaluation of this transistor amplifier. The available limit of noise figure at I_c=2mA, V_c=-6 volts is 7.49 (db), which can be realized by using the source impedance of 84-j13 (Ω). The experimental results of F_e of the amplifier which has the source impedance to optimize at I_c=2mA is 7.9 (db). This value almost agrees with the theoretical available limit. The numerical values mentioned here are only the examples. Some difference among the samples of transistor are recognized in the series of experiments.

5.12 Summary of Chapter V

The theoretical considerations on the exchangeable power gain and noise measure of linear active two-port by use of circuit parameters and its appli-

cation to transistor amplifiers are described in this chapter. The determination of stationary values of exchangeable power gain and their realization method using the eigenvalues and eigenvectors of the characteristic gain matrix which is defined in this chapter are presented. These stationary values agree with the well known complex conjugate matching power gain. Then, it is pointed out that there is the formal similarity between the solution of exchangeable power gain and that of the exchangeable noise measure of Haus and Adler. It is clarified that the characteristic gain matrix is singular for the unilateral two-port. Finally, by introducing the families of circles for constant exchangeable power gain and noise measure on the source impedance plane, the theory for the estimation of gain and noise performance in a general linear amplifier and for the designing its input circuit is developed from the view point of keeping the noise measure optimum. The above mentioned analytical method is also applied for the exchangeable excess noise figure.

CHAPTER VI CONCLUSION

After the investigations on the power gain and noise performance of linear active two-port by use of the circuit parameters, the following conclusions have been obtained.

1) The unilateral gain of Mason is represented in terms of Y,H,G,F and T parameters. It is also shown that the unilateral gain of transistor unit is an invariant with regard to its grounding methods after the comparison with the calculated results using the equivalent circuit. A kind of lossless transformation matrix for each permutation of grounding method is given. The calculated values of unilateral gain of transistor from its measured H parameters are shown in several operating conditions.

2) The input and output immittance chart with which it is able to find out graphically the input (or output) immittance, for the specified load (or source) immittance, and the load (or source) immittance for the specified input (or output) immittance is presented. This chart may be used more generally than the chart of Linvill.

3) There is the potentiality of designing the stable amplifier outside the Linvill chart when $ReH_{22} < 0$, which may result by use of the heavily positive feedback. The Linvill chart is extended toward the region of $G_L ReH_{22} < 0$ in order to generalize the design theory for all potential cases.

4) The power gain chart used with the extended Linvill chart is developed. The circuit designer is able to realize the maximum power gain of a given two-port, and to find the stable region of an amplifier for the specified terminations and the power gain in this stable region from this chart. The change of the power gain and stability due to the change of operating point is conveniently illustrated in this chart.

5) The graphical design method of high frequency transistor amplifiers, which does not depend on a particular equivalent circuit, is proposed based on the analysis of linear active two-port by means of the power gain chart, and the justification of this method is verified experimentally by considering the actual designs at VHF band.

6) The families of circles for constant power transfer ratio at the input and output of amplifier is introduced. These families of circles may be used on the estimation of mismatching effect of amplifiers and on the determination of bandwidth of tuned amplifiers if the changes of some of Z_S, Z_{in}, Y_{out}, and Y_L are not significant inside the bandwidth.

7) The relations between several noisy components in terms of power spectrum are formulated. These formulae are used in order to transform the two-port noise sources each other or to measure the set of them.

8) Though the two-port noise sources have been often used in the noise analysis of amplifier, we have no general measuring method except for the low frequency vacuum tube. The method to measure the two-port noise sources is developed here and the two-port noise of transistor is measured by this method, with the agreement to the values calculated from the theory of van der Ziel.

9) The eigenvalue of characteristic gain matrix which is defined in this thesis is the complex conju-

gate matching power gain of linear active two-port and the source impedance to realize it, is determined by the ratio of the components of its eigenvector. Moreover, it is pointed out that the stationary values and the source impedances to realize them can be obtained by the similar method for the exchangeable power gain, noise measure and noise figure, because they are expressed in the ratios of Hermitian form.

10) The loci of infinite exchangeable power gain and noise measure are the circles on the source impedance plane. As the circle of infinite exchangeable noise measure coincides with the locus (circle) of unity exchangeable power gain, the source impedances inside the circle that give the larger exchangeable power gain and the smaller exchangeable noise measure, must be used at the design of an amplifier with the positive source resistance.

11) The loci of constant exchangeable power gain, noise measure and noise figure form the families of circles on the source impedance plane. After drawing the families of circles and their cross sections for a given linear active two-port, one can readily use them for the estimation of amplifier gain and noise

performances or for the designing of amplifier input circuit.

12) The loci of the centers of circles for constant exchangeable power gain and noise measure are the straight lines. The former is parallel with the real axis of source impedance plane and the latter has a gradient to it. If the source impedance should be changed, it is preferable to move toward the proper direction along these straight lines, so that the resulting decreases of power gain and noise measure are not so significant.

- REFERENCES -

(1) S.J. Mason, "Power Gain in Feedback Amplifiers," IRE Trans. on Circuit Theory, vol. CT-1, pp. 20-25; June, 1954.

(2) S.J. Mason, "Power Gain in Feedback Amplifiers," Tech. Repts. MIT, no. 257; August, 1953.

(3) S.J. Mason, "Criteria for Docile Behavior of Feedback Amplifiers," Tech. Repts. MIT, no. 258; June, 1954.

(4) S.J. Mason, "Docile Behavior of Feedback Amplifiers," Proc. IRE, vol 44, pp. 781-787; June, 1956.

(5) R. L. Pritchard, "High Frequency Power Gain of Junction Transistors," Proc. IRE, vol. 43, pp. 1075-1085; September, 1955.

(6) A.P. Stern, "Stability and Power Gain of Tuned Transistor Amplifiers," Proc. IRE, vol. 45, pp. 335-343; March, 1957.

(7) E.F. Bolinder, "Survey of Some Properties of Linear Networks," IRE Trans. on Circuit Theory, vol. CT-4, pp. 70-78; September, 1957.

(8) G.E. Sharpe, J.L. Smith and J.R.W. Smith, "A Power Theorem on Absolutely Stable Two-ports," IRE Trans. on Circuit Theory, vol. CT-6, pp. 159-163; June, 1959.

(9) H.A. Haus and R.B. Adler, "Invariants of Linear Networks," 1956 IRE Convention Record, Part 2, pp. 53-67; 1956.

(10) H.A. Haus and R.B. Adler, "An Extention of the Noise Figure Definition," Proc. IRE, vol. 45, pp. 690-691; May, 1957.

(11) H.A. Haus and R.B. Adler, "Optimum Noise Performance of Linear Amplifiers," Proc. IRE, vol. 46,

pp. 1517-1533; August, 1958.

(12) H.A. Haus and R.B. Adler, "Network Realization of Optimum Amplifier Noise Performance," IRE Trans. on Circuit Theory, vol. CT-5, pp. 156-161; September, 1958.

(13) H.A. Haus and R.B. Adler, "Canonical Form of Linear Noisy Networks," IRE Trans. on Circuit Theory, vol. CT-5, pp. 161-167; September, 1958.

(14) H.A. Haus and R.B. Adler, "Circuit Theory of Linear Noisy Networks," John Wiley and Sons, Inc., New York, N.Y.; 1959.

(15) P. Penfield, Jr., "Noise in Negative Resistance Amplifiers," IRE Trans. on Circuit Theory, vol. CT-7, pp. 166-170; June, 1960.

(16) K. Kurokawa, "Actual Noise Measure of Linear Amplifiers," Proc. IRE, pp. 1391-1397; September, 1961.

(17) H. Heffner, "The Fundamental Noise Limit of Linear Amplifiers," Proc. IRE, vol. 50, pp. 1604-1608; July, 1962.

(18) J.G. Linvill and L.G. Schimpf, "The Design of Tetrode Transistor Amplifiers," Bell Sys. Tech. J., vol. 35, pp. 813-840; July, 1956.

(19) J.G. Linvill and J.F. Gibbons, "Transistors and Active Circuits," McGraw-Hill Book Company, New York; 1961.

(20) A.J. Cote Jr. and J.B. Oakes, "Linear Vacuum-tube and Transistor Circuits," McGraw-Hill Book Company, New York; 1961.

(21) D.J.R. Stock and L.J. Kaplan, "The Geometry of Representations for Active Networks," AEÜ, Band 16, Heft 5, pp. 223-226; 1962.

(22) C.M. Gewertz, "Synthesis of a Finite Four-terminal Network from its Prescribed Driving-point Functions

and Transfer Function," J. Math. Phys., vol. 12, pp. 1-257; January, 1933.

(23) F.B. Llewellyn, "Some Fundamental Properties of Transmission Systems," Proc. IRE, vol. 40, pp. 271-283; March, 1952.

(24) A. van der Ziel, "Theory of Shot Noise in Junction Diodes and Junction Transistors," Proc. IRE, vol. 43, pp. 1639-1646; November, 1955.

(25) A. van der Ziel, "Theory of Junction Diode and Junction Transistor Noise," Proc. IRE, vol. 46, pp. 589-594; March, 1958.

(26) A van der Ziel, "Noise in Junction Transistors," Proc. IRE, vol 46, pp. 1019-1038; June, 1958.

(27) B. Schneider and M.J.O. Strutt, "Theory and Experiments on Shot Noise in Silicon P-N Junction Diodes and Transistors," Proc. IRE, vol. 47, pp 546-554; April, 1959.

(28) Per-Olov Leine, "On the Power Gain of Unilaterized Active Networks," IRE Trans. on Circuit Theory, vol. CT-8, pp. 357-358; September, 1961.

(29) C.C. Cheng, "Neutralization and Unilateralization, IRE Trans. on Circuit Theory, vol. CT-2, pp. 138-145; June, 1955.

(30) A.P. Stern, C.A. Aldridge, and W.F. Chow, "Internal Feedback and Neutralization of Transistor Amplifiers," Proc. IRE, vol. 43, pp. 838-847; July, 1955.

(31) G.Y. Chu, "Unilateralization of Junction Transistor Amplifiers at High Frequencies," Proc. IRE, vol. 43, pp. 1001-1006; August, 1955.

(32) A.J. Cote, Jr., "Evaluation of Transistor Neutralization Networks," IRE Trans. on Circuit Theory, vol. CT-5, pp. 95-103; June, 1958.

(33) K. Aoyagi, T. Namekawa and K. Hirano, Joint Convention Record for Institute related to the Electrical Engineering of Japan, Kansai Section, no. 1-4; October, 1961. (in Japanese)

(34) K. Hirano, T. Namekawa and K. Aoyagi, "Considerations on Power Gain and Noise Measure of Linear Active Two-port," Monograph of PGCT of IECE of Japan, CT. 63-27; March, 1964. (in Japanese)

(35) K. Aoyagi, T. Namekawa and K. Hirano, "Consideration on the Power Gain of Linear Active Two-port," Monograph of PGTR of IECE of Japan, TR. 63-24; October, 1963. (in Japanese)

(36) K. Aoyagi, T. Namekawa and K. Hirano, "Power Gain Chart of Linear Active Two-port and its Application to High Frequency Transistor Amplifiers," IEEE Trans. on Circuit Theory. (under contribution)

(37) K. Aoyagi, T. Namekawa and K. Hirano, Joint Convention Record for Institute related to the Electrical Engineering of Japan, no. 59; April, 1963. (in Japanese)

(38) K. Aoyagi, T. Namekawa, K. Hirano and K. Kawamura, Convention Record for Institute of Electrical Communication Engineers of Japan, no. 15, November, 1962. (in Japanese)

(39) K. Aoyagi, T. Namekawa and K. Hirano, "On the Circle Diagrams of Linear Active Networks," Technol. Repts. Osaka Univ., vol. 13, no. 539; March, 1963.

(40) K. Aoyagi, T. Namekawa and K. Hirano, "A Design Method of High Frequency Transistor Amplifiers," Technol. Repts. Osaka Univ., vol. 13, no. 570; October, 1963.

(41) K. Aoyagi, T. Namekawa, K. Hirano and Y. Konba, Joint Convention Record for Institute related to the Electrical Engineering of Japan, Kansai Section, no. 17-9; November, 1964. (in Japanese)

(42) K. Aoyagi, T. Namekawa, K. Hirano and K. Tanaka, Joint Convention Record for Institute related to the Electrical Engineering of Japan, no. 1415; April, 1964. (in Japanese)

(43) K. Aoyagi, T. Namekawa, K. Hirano and K. Kusunoki, Convention Record for Institute of Electrical Communication Engineers of Japan, no. 415; November, 1964. (in Japanese)

(44) H. Rothe and W. Dahlke, "Theorie Rauschender Vierpole," AEÜ, Band 9, pp. 391-401; 1955.

(45) H. Rothe and W. Dahlke, "Theory of Noisy Fourpoles, Proc. IRE, pp. 811-817; June, 1956.

(46) T. Namekawa, "Studies on Vacuum-tube Noise and Noise Figure," Doctor Thesis of Osaka University; October, 1961. (in Japanese)

(47) K. Aoyagi, T. Namekawa and K. Hirano, "Studies on Power Gain and Noise Measure of Linear Active Two-port," presented at the ICMCI, C12-3, Tokyo; September, 1964.

(48) K. Aoyagi, T. Namekawa and K. Hirano, "Studies on Power Gain and Noise Measure of Linear Active Two-port," Journal of IECE of Japan. (under contribution)

(49) T. Namekawa, "On the Noise Figure of Low Gain Stages of Amplifiers and its Measurements," Journal of IECE of Japan, vol. 43, pp. 1329-1334; November, 1960. (in Japanese)

(50) K. Aoyagi, T. Namekawa and K. Hirano, Convention Record for Institute of Electrical Communication Engineers of Japan, no. 21; November, 1961. (in Japanese)

(51) K. Aoyagi, T. Namekawa and K. Hirano, Joint Convention Record for Institute related to the Electrical Engineering of Japan, no. 26; April, 1962. (in Japanese)

(52) K. Aoyagi, T. Namekawa and K. Hirano, Joint Convention Record for Institute related to the Electrical Engineering of Japan, Kansai Section, no. 1-10; November, 1962. (in Japanese)